JNeurosci Accepted Manuscript

JNeurosci
THE JOURNAL OF NEUROSCIENCE

Research Articles: Behavioral/Cognitive

Human somatosensory cortex is modulated during motor planning

https://doi.org/10.1523/JNEUROSCI.0342-21.2021

Cite as: J. Neurosci 2021; 10.1523/JNEUROSCI.0342-21.2021

Received: 13 February 2021
Revised: 11 May 2021
Accepted: 13 May 2021

This Early Release article has been peer-reviewed and accepted, but has not been through the composition and copyediting processes. The final version may differ slightly in style or formatting and will contain links to any extended data.

Alerts: Sign up at www.jneurosci.org/alerts to receive customized email alerts when the fully formatted version of this article is published.

Copyright © 2021 the authors

JNeurosci Accepted Manuscript

Human somatosensory cortex is modulated during motor planning

Daniel J. Gale[1], J. Randall Flanagan[1,2], & Jason P. Gallivan*[1,2,3]

[1]Centre for Neuroscience Studies, [2]Department of Psychology, and [3]Department of Biomedical and Molecular Sciences, Queen's University, Kingston, Ontario, Canada.

Abbreviated Title: Motor planning modulates somatosensory cortex

# of Pages: 36
# of Figures: 4
words in Abstract: 250
words in Introduction: 635
words in Discussion: 1789

*Correspondence should be addressed to:
Jason Gallivan
Centre for Neuroscience Studies
Queen's University
gallivan@queensu.ca

JNeurosci Accepted Manuscript

Abstract

Recent data and motor control theory argues that movement planning involves preparing the neural state of primary motor cortex (M1) for forthcoming action execution. Theories related to internal models, feedback control, and predictive coding also emphasize the importance of sensory prediction (and processing) prior to (and during) the movement itself, explaining why motor-related deficits can arise from damage to primary somatosensory cortex (S1). Motivated by this work, here we examined whether motor planning, in addition to changing the neural state of M1, changes the neural state of S1, preparing it for the sensory feedback that arises during action. We tested this idea in two human functional MRI studies (N=31, 16 female) involving delayed object manipulation tasks, focusing our analysis on pre-movement activity patterns in M1 and S1. We found that the motor effector to be used in the upcoming action could be decoded, well before movement, from neural activity in M1 in both studies. Critically, we found that this effector information was also present, well before movement, in S1. In particular, we found that the encoding of effector information in area 3b (S1 proper) was linked to the contralateral hand, similarly to that found in M1, whereas in areas 1 and 2 this encoding was present in both the contralateral and ipsilateral hemispheres. Together, these findings suggest that motor planning not only prepares the motor system for movement, but also changes the neural state of the somatosensory system, presumably allowing it to anticipate the sensory information received during movement.

Significance Statement

Whereas recent work on motor cortex has emphasized the critical role of movement planning in preparing neural activity for movement generation, it has not investigated the extent to which planning also modulates the activity in adjacent primary somatosensory cortex (S1). This reflects a key gap in knowledge, given that recent motor control theories emphasize the importance of sensory feedback processing in effective movement generation. Here we find, through a convergence of experiments and analyses, that the planning of object manipulation tasks, in addition to modulating the activity in motor cortex, changes the state of neural activity in different subfields of human S1. We suggest that this modulation prepares S1 for the sensory information it will receive during action execution.

Keywords

Motor, Planning, Somatosensory, Object manipulation, Action

JNeurosci Accepted Manuscript

INTRODUCTION

Motor planning has long been known to improve movement reaction time, speed, and accuracy (Keele, 1968; Klapp and Erwin, 1976; Rosenbaum, 1980; Wong et al., 2015; Haith et al., 2016). Consequently, a major focus of neural investigations in the field of motor control has been studying the changes in motor cortical activity that precede movement, and how this relates to various parameters (e.g., direction, extent, speed, curvature, force) of the forthcoming movement to be executed (Tanji and Evarts, 1976; Riehle and Requin, 1989; Hocherman and Wise, 1991; Shen and Alexander, 1997; Messier and Kalaska, 2000; Churchland et al., 2006b; Pesaran et al., 2006; Batista et al., 2007). Recent theories have argued that motor planning involves preparing the neural state of the motor system for upcoming movement execution, and have drawn links between how changes in neural population activity drive subsequent muscle activity (Shenoy et al., 2013). This work has enhanced our understanding, at the neural level, of how motor cortex generates movement, and has highlighted the importance of preparatory activity in setting up the state of motor system for this to occur (Churchland et al., 2006a; Churchland and Shenoy, 2007; Afshar et al., 2011; Ames et al., 2014).

Separately from the motor-related process of generating movement, a key component to successful motor control is the prediction and processing of the sensory consequences of action (Wolpert and Flanagan, 2001). For example, the sensorimotor control of object manipulation tasks involves predicting sensory signals associated with object contact events (e.g., object lift-off, replacement, etc.), which can occur in multiple sensory modalities, including tactile, proprioceptive and visual (Johansson and Flanagan, 2009). By comparing the expected to the actual sensory events that are experienced, the central nervous system can monitor task progression, detect performance errors, and quickly launch appropriate, task-protective corrective actions as needed (Johansson and Flanagan, 2009). The anticipation of the sensory consequences of action has long been theorized to rely on an efference copy of motor commands being sent from the motor cortex to the relevant sensory cortices (Holst et al., 1950; Crapse and Sommer, 2008). Consistent with this idea, work from both rodents and nonhuman primates has demonstrated that the motor cortex sends direct projections to the somatosensory system (Porter and White, 1983; Darian-Smith et al., 1993; Miyashita et al., 1994; Burton and Fabri, 1995; Cauller et al., 1998; Huffman and Krubitzer, 2001; Kinnischtzke et al., 2014), and

JNeurosci Accepted Manuscript

that these motor inputs can shape neural responses in primary somatosensory cortex, S1 (Jiang et al., 1990a; Lee et al., 2008; Zagha et al., 2013; Khateb et al., 2017; Umeda et al., 2019).

Given the behavioural importance of predicting task-specific tactile consequences during object manipulation tasks, here we hypothesized that action planning, in addition to preparing motor areas for execution (Shenoy et al., 2013), involves preparing S1 for the anticipated task-specific somatosensory signals. Because these sensory signals should change depending on the exact action to be executed, we would predict that, as is the case in the motor system (Porter and Lemon, 1995; Gallivan and Culham, 2015a), planning-related modulations in S1 should exhibit the hallmarks of contralaterality and effector specificity, and perhaps also differentiation according to hierarchical organization (i.e., changes in informational content across lower-to-higher order S1 subareas).

To explore these ideas in humans, here we examined, using functional MRI in two separate experiments involving delayed object lifting tasks, whether the upcoming actions to be performed by an individual are represented in delay period activity in S1. In both studies, we find that information related to the motor effector to be used can be decoded from pre-movement activity patterns in different subareas of human S1. These findings suggest that motor planning changes the neural state of somatosensory cortex based on the movement being prepared, perhaps readying it to extract task-related sensory information during the unfolding movement.

MATERIALS & METHODS

Overview

To test whether and how the motor preparation of object manipulation tasks changes the neural state of somatosensory cortex, we performed new analyses on two recently published datasets (Gale et al., 2021). In brief, both experiments used delayed movement tasks, allowing us to separate out motor planning-related modulations in somatosensory cortex from the later sensory feedback-related modulations that occur during movement execution. In the first experiment, each trial had participants first prepare, and then execute either a left or right hand object lift-and-replace action (these movements were cued via two nonsense auditory commands, see Fig. 1A,B). In the second experiment, each trial had participants first prepare, and then execute either a right hand object lift-and-replace action or a target-directed eye movement (these movements were cued via a change in the colour of a central fixation light,

JNeurosci Accepted Manuscript

see Fig. 1D,E). Both of these experiments allowed us to examine whether human somatosensory cortex, during the delay period prior to movement, encodes the upcoming motor effector to be used (left versus right hand in Experiment 1, and right hand versus eye in Experiment 2). Such a result would provide evidence that the neural state of somatosensory cortex is modulated prior to movement execution.

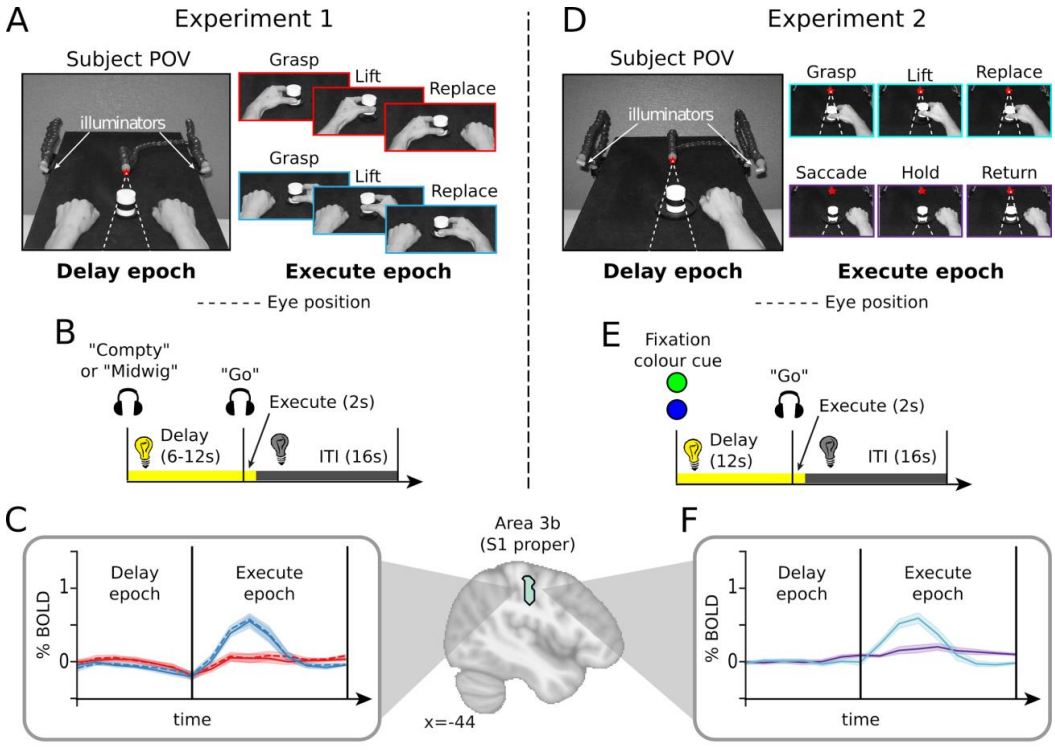

Figure 1. Overview of the two experiments.
A. Experiment 1 task. Subject point-of-view (POV, left) of the experimental workspace during the Delay epoch. Red star indicates the fixation LED placed above the object. Illuminator LEDs, attached to flexible stalks, are shown on the left and right. During the Execute epoch (right), subjects executed either an object grasp, lift-and-replace action with their left hand (red bordering) or right hand (blue bordering). During the study, subjects maintained central fixation on the fixation LED. **B and C.** Sequence of events in a single trial (B) and corresponding group-averaged (N=15) single-trial BOLD data (C) from left primary somatosensory cortex area BA3b (S1 proper, cyan region), time-locked to events in B. Each trial begins with the hand workspace being illuminated while, simultaneously, participants receive the auditory cue ("Compty" or "Midwig"). This auditory cue instructs either a left or right hand action (based on the mapping given to participants, see Methods). This is then followed by a jittered 6-12s Delay interval. Next, an auditory "Go" cue initiates the start of the 2s Execute epoch, during which the subject grasps, lifts and replaces the object. Following the 2 s Execute epoch, illumination of the workspace is extinguished and subjects then wait a fixed 16s intertrial interval (ITI) prior to onset

JNeurosci Accepted Manuscript

of the next trial. **D.** Experiment 2 task. Subject POV during the Delay (left) and Execute (right) epochs. During the Execute epoch subjects executed either an object grasp, lift-and-replace action with their right hand (cyan bordering) or an object-directed saccadic eye movement (purple bordering). Other than the saccadic eye movement, subjects maintained central fixation on the fixation LED during all other phases of the trial, as in Experiment 1. **E and F.** Sequence of events in a single-trial (E) and corresponding group-averaged (N=13) single-trial BOLD data (F) from BA3b in the left hemisphere, time-locked to events in E. In both C and F, note that left BA3b is primarily modulated by movements on the contralateral (right hand) during the Execute epoch.

Participants

Sixteen healthy right-handed subjects (8 females, 21-25 years of age) participated in Experiment 1 and a separate cohort of fifteen healthy right-handed subjects (8 females, 20-32 years of age) participated in Experiment 2. All experiments were undertaken with the understanding and written consent of each subject, obtained in accordance with ethical standards set out by the Declaration of Helsinki (1964) and with procedures cleared by the Queen's University Health Sciences Research Ethics Board. Data from one subject in Experiment 1 and from two subjects in Experiment 2 were excluded from further analyses due to data collection problems in the experimental testing sessions, resulting in final sample sizes of 15 and 13 subjects, respectively. The complete methods for Experiments 1 and 2 have recently been described in full detail elsewhere (Gale et al., 2021). As such, here we provide more concise descriptions of the methods relevant for our new analyses.

Experiment 1

Subjects were scanned in a head-tilted configuration (allowing direct viewing of the hand workspace) while they performed a delayed object lift-and-replace task (see Fig. 1A,B for an overview of the experimental setup and timing). During the experiment, the participant's workspace was illuminated by two bright white Light Emitting Diodes (LEDs) attached to flexible plastic stalks. To control for eye movements, a small red fixation LED, attached to a flexible plastic stalk, was positioned above the hand workspace. Experimental timing and lighting were controlled with in-house software created with C++ and MATLAB (The Mathworks, Natnick, MA). Throughout fMRI testing, the subject's hand movements were monitored using an MR-compatible infrared-sensitive camera, optimally positioned on one side of the platform and facing towards the subject. The videos captured during the experiment were analyzed offline to verify that the subjects were performing the task as instructed and to identify error trials (e.g., performing the wrong action, moving the hand before the Execute epoch).

JNeurosci Accepted Manuscript

On each trial, subjects were required to perform one of two actions upon a centrally located target object: (1) grasp, lift and replace the object with the left hand and (2) grasp, lift and replace the object with the right hand (see Fig. 1A). These actions were cued via two nonsense speech cues, “Compty” or “Midwig”. For a given trial, each nonsense speech cue was paired with a corresponding hand action (i.e., subjects were instructed that, for a predetermined set of trials, “Compty” cued a left hand movement whereas “Midwig” cued a right hand movement). Halfway throughout the scan (following a “Switch” auditory cue), this cue-hand mapping was reversed (e.g., “Compty” would now cue a right hand movement whereas “Midwig” would now cue a left hand movement). Following the delivery of the auditory command, there was a jittered delay interval of 6-12 s (a Gaussian random jitter with a mean of 9 s), after which the verbal auditory command “Go” was delivered, prompting subjects to execute the prepared grasp, lift and replace action. For this execution phase of the trial, subjects were required to precision grasp-and-then-lift the object with their thumb and index finger (~2 cm above the platform, via a rotation of the wrist), hold it in midair for ~1 s, and then replace it. Two seconds following the onset of this “Go” cue, the illuminator lights were extinguished, and subjects then waited 16 s for the next trial to begin (intertrial interval, ITI). Throughout the entire time course of the trial, subjects were required to maintain gaze on the fixation LED and, other than the execution of the hand actions, participants were required to keep their hands still and in pre-specified “home” positions to the left and right of the central object.

This experiment resulted in a total of 4 different auditory-hand mappings (and thus, trial types) per experimental run: Compty-left hand, Compty-right hand, Midwig-left hand, and Midwig-right hand (with 5 repetitions each; 20 trials in total per run). With the exception of the blocked nature of these trials, these trial types were pseudorandomized within a run and counterbalanced across all runs so that each trial type was preceded and followed equally often by every other trial type across the entire experiment. For the purposes of the present analysis (i.e., focused on decoding motor effector-information from primary somatosensory cortex), we collapsed trials across auditory cue (“Compty” vs. “Midwig”) and only examined decoding with respect to hand information (left versus right).

During MRI testing, we also tracked subjects’ behaviour using an MRI-compatible force sensor located beneath the object (Nano 17 F/T sensors; ATI Industrial Automation, Garner, NC), and attached to our MRI platform. This allowed us to track both subject reaction time (RT), which we

JNeurosci Accepted Manuscript

define as the time from the onset of the “Go” cue to object contact (Mean = 1601ms, SD = 389ms), and movement time (MT), which we define as the time from object lift to replacement (Mean = 2582ms, SD = 662ms), as well as generally monitor task performance. Each subject participated in 8 functional runs (for a total of 160 trials; 80 trials for each hand). See Gale et al. for further details. Note that we did not conduct eye tracking during this experiment, nor in Experiment 2, due to difficulties in monitoring gaze in the head-tilted configuration with standard MRI-compatible eye trackers (due to occlusion from the eyelids). Nevertheless, behavioural control experiments have demonstrated that the same groups of subjects tested with MRI can reliably maintain fixation during behavioural testing (Gale et al., 2021).

Experiment 2

This study was similar to Experiment 1, with the exception that: (1) participants performed either a right hand object grasp-and-lift action on the centrally located object or a target-directed eye movement towards that same object (i.e., two experimental conditions, see Fig 1D), (2) the Delay epoch was a fixed duration (12 s), and (3) subjects were cued about the upcoming movement to be executed via a 0.5 s change in the fixation LED colour (from red to either blue or green, with the colour-action mapping being counterbalanced across subjects; i.e., a LED change to blue cued a grasp action in half the subjects, and cued an eye movement in the other half of subjects). The eye movement action involved the subject making a saccadic eye movement from the fixation LED to the target object, holding that position until the illuminator LEDs were extinguished, and then returning their gaze back to the fixation LED. The two trial types, with 5 repetitions per condition (10 trials total per run), were pseudorandomized as in Experiment 1. Each subject participated in at least eight functional runs (thus creating 40 repetitions per condition across the experiment).

Data Acquisition and Analysis

Subjects were scanned using a 3-Tesla Siemens TIM MAGNETOM Trio MRI scanner located at the Centre for Neuroscience Studies, Queen’s University (Kingston, Ontario, Canada). An identical imaging protocol was used for both Experiments 1 and 2, with the exception of slice thickness (Experiment 1 = 4mm; Experiment 2 = 3mm). In both experiments, MRI volumes were acquired using a T2*-weighted single-shot gradient-echo echo-planar imaging acquisition sequence (time to repetition = 2000 ms, in-plane resolution = 3 mm x 3 mm, time to echo = 30 ms, field of view = 240 mm x 240 mm, matrix size = 80 x 80, flip angle = 90°, and acceleration factor (integrated parallel acquisition technologies, iPAT) = 2 with generalized auto-calibrating

JNeurosci Accepted Manuscript

partially parallel acquisitions reconstruction). Each volume comprised 35 contiguous (no gap) oblique slices acquired at a ~30° caudal tilt with respect to the plane of the anterior and posterior commissure (AC-PC). Subjects were scanned in a head-tilted configuration, allowing direct viewing of the hand workspace. We used a combination of imaging coils to achieve a good signal to noise ratio and to enable direct object workspace viewing without mirrors or occlusion. Specifically, we tilted (~20° degrees) the posterior half of the 12-channel receive-only head coil (6-channels) and suspended a 4-channel receive-only flex coil over the anterior-superior part of the head. An identical T1-weighted ADNI MPRAGE anatomical scan was also collected for both Experiments 1 and 2 (time to repetition = 1760 ms, time to echo = 2.98 ms, field of view = 192 mm x 240 mm x 256 mm, matrix size = 192 x 240 x 256, flip angle = 9°, 1 mm isotropic voxels).

fMRI data preprocessing

Preprocessing of functional data collected in Experiments 1 and 2 was performed using *fMRIPrep* 1.4.1 (Esteban et al., 2018), which is based on *Nipype* 1.2.0 (Gorgolewski et al., 2011; Esteban et al., 2019).

Anatomical data preprocessing

The T1-weighted (T1w) image was corrected for intensity non-uniformity (INU) with N4BiasFieldCorrection (Tustison et al., 2010), distributed with ANTs 2.2.0 (Avants et al., 2008), and used as T1w-reference throughout the workflow. The T1w-reference was then skull-stripped with a Nipype implementation of the antsBrainExtraction.sh workflow (from ANTs), using OASIS30ANTs as target template. Brain tissue segmentation of cerebrospinal fluid (CSF), white-matter (WM) and gray-matter (GM) was performed on the brain-extracted T1w using fast (FSL 5.0.9, (Zhang et al., 2001)). Brain surfaces were reconstructed using recon-all (FreeSurfer 6.0.1, (Dale et al., 1999)), and the brain mask estimated previously was refined with a custom variation of the method to reconcile ANTs-derived and FreeSurfer-derived segmentations of the cortical gray-matter of Mindboggle (Klein et al., 2017). Volume-based spatial normalization to standard space, FSL's MNI ICBM 152 non-linear 6th Generation Asymmetric Average Brain Stereotaxic Registration Model [(Evans et al., 2012); TemplateFlow ID: MNI152NLin6Asym], was performed through nonlinear registration with antsRegistration (ANTs 2.2.0), using brain-extracted versions of both T1w reference and the T1w template.

JNeurosci Accepted Manuscript

Functional data preprocessing

For each BOLD run per subject (across all tasks and/or sessions), the following preprocessing was performed. First, a reference volume and its skull-stripped version were generated using a custom methodology of fMRIPrep. The BOLD reference was then co-registered to the T1w reference using bbregister (FreeSurfer) which implements boundary-based registration (Greve and Fischl, 2009). Co-registration was configured with nine degrees of freedom to account for distortions remaining in the BOLD reference. Head-motion parameters with respect to the BOLD reference (transformation matrices, and six corresponding rotation and translation parameters) are estimated before any spatiotemporal filtering using mcflirt (FSL 5.0.9, (Jenkinson et al., 2002)). BOLD runs were slice-time corrected using 3dTshift from AFNI 20160207 (Cox and Hyde, 1997). The BOLD time-series were normalized by resampling into standard space (voxel size = 2 × 2 × 2 mm). All resamplings were performed with a single interpolation step by composing all the pertinent transformations (i.e. head-motion transform matrices, and co-registrations to anatomical and output spaces). Gridded (volumetric) resamplings were performed using antsApplyTransforms (ANTs), configured with Lanczos interpolation to minimize the smoothing effects of other kernels (Lanczos, 1964).

Many internal operations of fMRIPrep use Nilearn 0.5.2 (Abraham et al., 2014), mostly within the functional processing workflow. For more details of the pipeline, see the section corresponding to workflows in fMRIPrep's documentation.

Error trials

Error trials involving the hand were identified offline from the videos recorded during the experimental testing session and were excluded from analysis by assigning these trials predictors of no interest. Error trials included those in which the subject performed the incorrect instruction (Experiment 1: 9 trials, 4 subjects; Experiment 2: 1 trial, 1 subject) or contaminated the delay epoch data by slightly moving their limb or moving too early (Experiment 1: 7 trials, 4 subjects; Experiment 2: 1 trial, 1 subject). Note that, due to our inability to record gaze during MRI testing (see Experiment 1, above), error trials involving eye movements could not be identified and excluded from our analysis.

JNeurosci Accepted Manuscript

Statistical Analyses

General Linear Models

We employed a Least-Squares Separate procedure (Mumford et al., 2012) to extract beta coefficient estimates for decoding analyses. This procedure generated separate GLM models for each individual trial's Delay and Execute epochs (e.g., In Experiment 1: 20 trials x 2 epochs x 8 runs = 320 GLMs). The regressor of interest in each model consisted of a boxcar regressor aligned to the start of the epoch of interest. The duration of the regressor was set to the duration of the cue that initiates the epoch (0.5s): the auditory command cue ('Compty' or 'Midwig') and the visual cue (fixation LED colour change) for the Delay epoch in Experiment 1 and 2, respectively; and the auditory 'Go' cue for the Execute epoch in both experiments. For each GLM, we included a second regressor comprised of all the remaining trial epochs in the experimental run. Each regressor was then convolved with a double-gamma HRF, and temporal derivatives of both regressors were included along with subjects' six motion parameters obtained from motion correction. High-pass filtering was added to each design matrix by the inclusion of regressors from a cosine drift model with a cutoff of 0.01 Hz. Isolating the regressor of interest in this single-trial fashion reduces regressor collinearity, and has been shown to be advantageous in estimating single-trial voxel patterns and for multi-voxel pattern classification (Mumford et al., 2012). These procedures were implemented using Nistats 0.0.1b1 and Nilearn 0.6.0 (Abraham et al., 2014).

We performed additional GLM contrast analyses to place our searchlight results (see Searchlight Pattern-Information Analyses) in the context of univariate activity elicited by each effector (i.e. Experiment 1: left and right hand; Experiment 2: eye and right hand) during movement execution. At the subject level, Delay and Execute epochs for each condition were modelled as separate regressors (Experiment 1: Left-Delay, Left-Execute, Right-Delay, Right-Execute; Experiment 2: Look-Delay, Look-Execute, Grasp-Delay, Grasp-Execute), with onsets aligned to the start of each epoch and durations of 0.5 s for the Delay and Execute epochs (consistent with our single trial GLMs described above). Group-level Execute > Delay contrasts for each effector in each experiment were performed on smoothed subject-level parameter maps (Gaussian kernel FWHM = 6mm). Contrasting the Execute vs Delay epoch within each condition rather than Execute epochs between conditions (i.e. Experiment 1: Left Execute vs Right Execute; Experiment 2: Look Execute vs Grasp Execute) enables us to show activity

JNeurosci Accepted Manuscript

maps elicited by each effector separately, rather than activity maps that directly compare the effectors to each other.

Region of interest (ROI) selection

Regions of interest (ROIs) for human primary somatosensory cortex (S1) were defined using region masks for Brodmann's areas (BA) 3a, 3b, 1 and 2 (Brodmann, 1909; Vogt and Vogt, 1919) from the Jülich histological (cyto- and myelo-architectonic) atlas (Geyer et al., 1999; Grefkes et al., 2001). Each non-overlapping region mask was based off of a 25% probability threshold for each region, which is packaged by default in FSL 5.0.10 (Jenkinson et al., 2012). We considered these four subdivisions of S1 separately since they are considered distinct functional areas, and are thought to be positioned at different hierarchical stages of somatosensory processing (Kaas, 1983; Geyer et al., 1999). BA3b, which receives dense inputs from the ventroposterior (VP) nucleus of the thalamus, is often considered 'S1 proper' as it primarily responds to cutaneous input (Kaas, 1983). BA3a also receives dense inputs from the thalamus, but is thought to be primarily concerned with proprioceptive processing, due to its deep (subcutaneous) receptor inputs (i.e., from muscle spindle afferents). The status of BA3a as part of primary somatosensory cortex is debatable, as many neuroanatomists regard it as part of BA4 (primary motor cortex)(Jones et al., 1978; Vogt and Pandya, 1978; Kaas, 1983). BA1 receives significant projections from BA3b and is thought to be concerned with texture-related processing, whereas BA2 receives significant projections from BA3a and 1 and is thought to be concerned with size/shape-related processing (Randolph and Semmes, 1974; Jones et al., 1978; Vogt and Pandya, 1978; Kaas, 1983; Pons and Kaas, 1986). Thus, BA1 and 2 are thought to be positioned at a slightly higher 'hierarchical' level than BA3b. [*We recognize that some researchers will take issue with our description of S1 as containing several different subfields (BA3a, BA3b, BA1 and BA2), as many neuroanatomists use the 'S1' nomenclature to denote BA3b specifically (Kaas, 1983). However, in most fMRI studies, the delineation of these different subfields is not typically performed, and 'primary somatosensory cortex' or area 'S1' terminology is often used interchangeably to distinguish dorsomedial activity located on or near the postcentral gyrus from 'secondary somatosensory cortex' or 'S2' activity that is located on the same gyrus but more laterally, in the parietal operculum (Eickhoff et al., 2006a, 2006b, 2007). Given our use of fMRI in the current study, we have adopted the latter naming conventions, but appreciate that the separate BA3a, BA3b, BA1 and BA2 fields have different patterns of cytoarchitectonics, connections and physiological response properties (Jones et al., 1978; Vogt and Pandya, 1978; Kaas, 1983)*.]

JNeurosci Accepted Manuscript

We also defined ROIs for primary motor cortex (M1) in BA4a (4 anterior) and BA4p (4 posterior) (Brodmann, 1909; Vogt and Vogt, 1919), also from the Jülich histological (cyto- and myelo-architectonic) atlas (Geyer et al., 1996) based on the same 25% probability threshold. These are known areas involved in motor planning and execution (Kalaska, 2009), and thus serve as a basis for comparing and interpreting the effects observed in the S1 ROIs above. Together, the above sets of S1 and M1 ROIs were used as three-dimensional binary masks to constrain our neural decoding analyses and interpretations of motor planning-related effects across the postcentral and precentral gyri.

Multi-voxel Pattern Analysis (MVPA)

MVPA was performed with in-house software using Python 3.7.1 with Nilearn 0.6.0 and Scikit-Learn 0.20.1 (Abraham et al., 2014). All analyses implement linear support vector machine (SVM) binary classifiers using Scikit-Learn's LinearSVC, which implements LIBLINEAR (Fan et al., 2008), with a fixed regulation parameter (C = 1) in order to compute a hyperplane that best separated the trial responses. The pattern of voxel beta coefficients from the single-trial GLMs, which provided voxel patterns for each trial's Delay and Execute epochs, were used as inputs into the binary classifiers.

Decoding accuracies for each subject were computed as the average classification accuracy across train-and-test iterations using a 'leave-one-run-out' cross-validation procedure. During each iteration, each voxel in the training set was standardized to have a mean of 0 and standard deviation of 1, and the test set was standardized based on the scaling parameters of the training set. This standardization approach maintains independence of training and test sets by ensuring that parameters from the test set do not influence model fitting on the training set (i.e. data leakage). The cross-validation procedure was performed separately for each ROI, trial epoch (Delay and Execute), and pairwise discrimination (left hand vs right hand movements in Experiment 1; and hand vs. eye movements in Experiment 2).

We assessed decoding significance at the group-level using a previously published two-step permutation procedure (Gale et al., 2021), which is based on permutation approaches outlined in (Stelzer et al., 2013). The first step generates, for each subject, a chance decoding distribution by repeatedly (100 iterations) computing the average classification accuracy of leave-one-run-out cross validation on randomly shuffled class labels within each run. The

JNeurosci Accepted Manuscript

second step computes a distribution of group mean decoding accuracies by repeatedly (10,000 iterations) selecting a random decoding accuracy from each subject's decoding distribution and computing the mean decoding accuracy across subjects. This distribution of group mean decoding accuracies was then used to compute the probability of the actual group mean decoding accuracy. Here, we used a one-tailed significance threshold of $p < .05$ and controlled for the problem of multiple comparisons (number of ROIs examined) by applying a Benjamini-Hochberg false-discovery rate (FDR) correction of $q < 0.05$.

Searchlight Pattern-Information Analyses

We performed confirmatory searchlight analyses for the Delay and Execute epochs in Experiments 1 and 2. To set the scope of the searchlight, we generated a searchlight mask by combining all somatosensory and motor ROIs and then dilating the mask by 1 voxel. Then, a searchlight sphere (4mm radius, 33 voxels) was applied to each voxel in the searchlight mask, and the cross-validation decoding procedure (see above) was performed on the extracted beta patterns produced by our GLM procedure. The decoding accuracy for each sphere of voxels was then written to the central voxel to generate a searchlight map. Searchlight maps for each subject were spatially smoothed (6mm FWHM Gaussian kernel) to facilitate group-level analyses (i.e. account for individual variability in localization). Because spatial smoothing reduces spatial precision in favour of spatial overlap across subjects, we also performed group-level analyses on unsmoothed searchlight maps, in which spatial overlap across subjects is reduced in favour of spatial precision. For each smoothed and unsmoothed data, subject searchlight maps were combined and one-tailed t-test versus 50% decoding (i.e. chance) was performed on each voxel, and the resulting group map was thresholded at $p < .001$. Together, this resulted in 8 total searchlight analyses (i.e. smoothed and unsmoothed versions for the Delay and Execute epochs in Experiments 1 and 2).

Each searchlight analysis was corrected for multiple comparisons using cluster-extent thresholds from a permutation approach based on Markiewicz and Bohland (2016), which provides a computationally feasible alternative to Stelzer et al. (2013) for searchlight permutation testing (see Gale et al. 2021 for a previous implementation). In this approach, 100 chance decoding maps for each subject are constructed by repeatedly applying our searchlight procedure with randomly shuffled class labels within each run. Then, a distribution of cluster sizes was generated by $10e^3$ iterations of a) selecting a random chance decoding map from each subject, b) performing one-tailed t-tests versus 50% decoding (chance) on each voxel, and

JNeurosci Accepted Manuscript

c) thresholding the map at $p < .001$ and extracting the sizes of all individual clusters. The cluster-extent threshold was then determined by taking the minimum cluster size at which $p < .05$. This procedure was performed separately for all searchlight analyses. For visualization purposes, the corrected thresholded searchlight maps were projected onto an fsaverage surface (Fischl et al., 1999) using an accurate registration-fusion procedure from Wu et al. (2018).

RESULTS

Experiment 1

Motor effector information is encoded in primary somatosensory cortex prior to movement

In Experiment 1, subjects performed a delayed object manipulation task (Fig. 1A) wherein they first prepared, and then executed, object grasp, lift-and-replace movements with their left or right hands. To determine whether primary somatosensory cortex (S1) encodes information related to the upcoming movements, we performed neural decoding on the trial-related voxel patterns (beta coefficients) associated with the Delay and Execute epochs from each of the four subareas that make up human S1: BA3a, BA3b, BA1 and BA2 (see Fig 2A). BA3b is considered S1 'proper' (Kaas, 1983), with areas BA1 and BA2 being considered slightly higher-order subdivisions (Jones et al., 1978; Vogt and Pandya, 1978; Pons and Kaas, 1986)(see also Methods). Decoding analyses (see Fig. 2B) revealed that information related to the upcoming hand actions to be performed (i.e., during the Delay epoch) was present in all 4 subareas of S1 in both the left and right hemispheres (*Left hemisphere*: BA3b: mean = 59.52%, $p < .001$; BA3a: mean = 56.56%, $p < .001$; BA1: mean = 60.22%, $p < .001$; BA2: mean = 57.95%, $p < .001$; *Right hemisphere*: BA3b: mean = 60.27%, $p = < .001$; BA3a: mean = 53.17%, $p = .003$; BA1: mean = 61.54%, $p < .001$; BA2: mean = 55.41%, $p < .001$; all p-values are FDR-corrected). In addition, consistent with the influx of tactile and proprioceptive sensory-related information during movement execution, we found that decoding in each of these subareas was substantially higher during the Execute epoch (decoding accuracies between 73% - 94%, all $p < .001$). Critically, our finding that decoding occurred in S1 during the Delay period (and not just Execute period) indicates that S1 subareas are modulated by the movement being prepared, but not yet executed. Consistent with this idea, a separate analysis on the classification accuracies for the decoding of auditory cue information (i.e., re-labelling all trials according to the "Compty" vs. "Midwig" auditory cues that instructed the movements, and thus collapsing across left vs. right hand trials) revealed no evidence for decoding across any of the S1

JNeurosci Accepted Manuscript

subareas in either hemisphere (*Left hemisphere*: BA3b: mean = 49.25%, p = .944; BA3a: mean = 51.30%, p = .676; BA1: mean = 47.81%, p = .944; BA2: mean = 48.56%, p = .944; *Right hemisphere*: BA3b: mean = 52.84%, p = .161; BA3a: mean = 51.10%, p = .852; BA1: mean = 50.65%, p = .916; BA2: mean = 48.10%, p = .944; all p-values are FDR-corrected). This importantly indicates that the significant decoding of the hand movements above was not spurious in nature, but instead specifically linked to the hand to be used in the upcoming action.

One possibility is that the jittering of the Delay epoch may have resulted in some subjects producing small anticipatory movements during the Delay epoch in anticipation of the Go cue. While we cannot definitively rule out such a possibility, we do not think this is a likely explanation of our decoding results for a few reasons. First, we failed to observe reliable evidence of pre-execute movements based on our video monitoring of subjects' hand movements during the task (and of those trials that were identified, 0.4% of all trials, they were removed from analysis). Second, we observed no association, across participants, between the Delay epoch duration and the movement execution reaction time, as might be expected from prior literature (Niemi and Näätänen, 1981). This suggests that subjects were not overly anticipating the 'Go' cue on the longer delay duration trials (e.g., trials in which the Delay epoch exceeded 9 s duration). Consistent with this, we also observed no differences in decoding magnitude between longer (>9 s) versus shorter (<9 s) delay duration trials. In summary, while we cannot exclude the possibility that subjects exhibited subthreshold hand/finger movements during the delay epoch, it is unlikely that such movements were linked to our ability to decode hand-related information prior to movement.

JNeurosci Accepted Manuscript

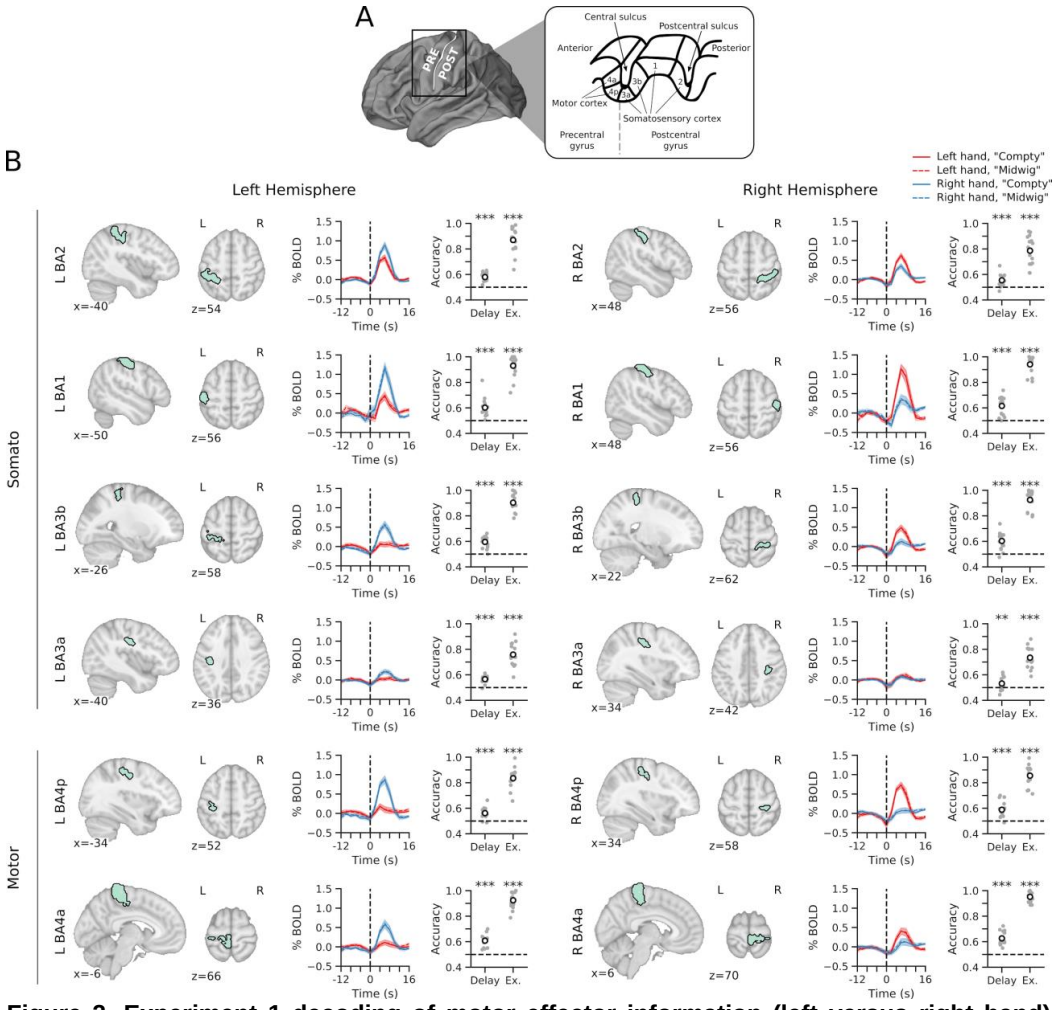

Figure 2. Experiment 1 decoding of motor effector information (left versus right hand) from early somatosensory cortex during the delay epoch. A. Lateral surface view of the human brain (at left), with the precentral and postcentral gyri demarcated (separated by the central sulcus, white line). Zoomed-in cross-sectional view of the precentral and postcentral gyri (at right), demarcating the different cytoarchitectonic subareas of M1 (BA4a and BA4p) and S1 (BA3a, BA3b, BA1 and BA2). Figure is adapted from (Borich et al., 2015). **B.** Each individual subarea arranged posterior to anterior, shown on sagittal and transverse brain slices, is associated with a group-averaged percent-signal change (%SC) BOLD time course and a decoding accuracy for hand information (point plots), separately for the Delay and Execute (Ex.) epochs. Left and right hemisphere S1 and M1 subareas are shown on the left and right, respectively. The %SC data is time-locked to the onset of the Execute epoch (vertical dashed line). In the decoding accuracy plots, black circles indicate mean decoding accuracy, and gray points show individual subject decoding accuracies. Chance level (50%) is demarcated by the horizontal dashed line in each decoding plot. Note that all subareas show significant decoding of hand information during the Delay epoch despite the high degree of overlap amongst the time courses for the different experimental conditions. Significance of hand decoding accuracies

JNeurosci Accepted Manuscript

were determined for each epoch using null decoding distributions derived via permutation tests (see Methods). Stars denote FDR-corrected significance levels (* $p < .05$, ** $p < .01$, *** $p < .001$). L = left; R = right.

Delay period decoding from somatosensory cortex is similar to that observed in motor cortex

To provide a basis for interpreting the S1 decoding results above, we also examined delay period decoding in two regions in the primary motor cortex (M1), BA4a and BA4p (see Methods). These areas served as 'positive control' regions, given that they are well known to differentiate limb-related information during movement planning in both humans and nonhuman primates (Cisek et al., 2003; Gallivan et al., 2013a). As expected, we observed significant decoding during the Delay epoch in both M1 areas in both the left and right hemispheres (*Left hemisphere*: BA4a: mean = 60.78%, $p < .001$; BA4p: mean = 56.17%, $p < .001$; *Right hemisphere*: BA4a: mean = 62.62%, $p < .001$; BA4p: mean = 58.83%, $p < .001$, all p-values are FDR-corrected, Fig. 2B). Unsurprisingly, decoding in both these areas was even more robust during the Execute epoch (decoding accuracies between 83% - 95%; all $p < .001$). These M1 findings not only offer proof of data quality but also provide initial evidence that similar levels of action-related information can be decoded from S1 as from M1 prior to movement.

Experiment 2

Our Experiment 1 results show that motor effector-related information (left vs. right hand) can be decoded from neural activity patterns in bilateral S1 prior to movement onset. What remains unclear from this first study, however, is the extent to which these S1 modulations are contralateral in nature. That is, because both hands were used in Experiment 1 and we observe decoding in both the left and right S1, we are unable to disentangle whether (1) the left somatosensory cortex *only* encodes upcoming movements of the right limb, and vice versa (i.e., a contralateral modulation) or, alternatively, (2) whether left (and right) somatosensory cortex is differentially modulated by planned movements of either limb (i.e., both a contra- and ipsi-lateral modulation). A separate delayed movement task in which only one of the limbs is used would allow us to directly examine whether, during the delay period, both the contralateral and ipsilateral somatosensory cortices (with respect to the limb) are modulated during planning.

To test this, as well as replicate and extend the general findings reported in Experiment 1, we performed a second experiment wherein we modified a classic task from primate

JNeurosci Accepted Manuscript

neurophysiology used to dissociate motor- versus sensory-related representations in the context of motor planning (Snyder et al., 1997; Cui and Andersen, 2007). In our variant of this delayed movement task, we had participants, in each trial, either grasp, lift-and-replace an object with their right hand or make a saccadic eye movement towards the object (Fig. 1D,E). If somatosensory cortex is modulated in a purely contralateral fashion, then we would expect that only the left somatosensory cortex will decode planned right hand versus eye movements; by contrast, if somatosensory cortex is modulated in both a contra- and ipsi-lateral fashion, then we would expect that both the left and right somatosensory cortex will decode planned right hand versus eye movements.

Movement preparation modulates BA3b in a contralateral fashion, but modulates higher-order areas BA1 and BA2 in a bilateral fashion

As in Experiment 1, a decoding analysis on Delay epoch voxel patterns revealed that information related to the upcoming effector to be used (hand vs. eye) could be decoded from S1 subareas (see Fig. 3). Notably, however, we found that the motor effector-decoding was not entirely bilateral. In the higher-order subareas BA1 and BA2, we found that hand information could be decoded from both the contralateral (*Left hemisphere*: BA1: mean = 63.17%, $p < .001$; BA2: mean = 59.04%, $p < .001$) and ipsilateral (*Right hemisphere*: BA1: mean = 55.58%, $p = .002$; BA2: mean = 56.83%, $p < .001$; all p-values are FDR-corrected) somatosensory cortex. In S1 proper, by contrast, we found that hand information could only be decoded from the contralateral somatosensory cortex (Left BA3b: mean = 57.98%, $p < .001$; Right BA3b: mean = 51.25%, $p = 0.335$; all p-values are FDR-corrected). We also observed no significant decoding from either left or right BA3a (*Left hemisphere*: BA3a: mean = 51.54%, $p = .235$; *Right hemisphere:* BA3a: mean = 49.52%, $p = .628$; all p-values are FDR-corrected). However, during the Execute epoch, as in Experiment 1, we found that effector-related decoding was robust in all four subareas in both hemispheres (decoding accuracies between 58% - 83%, all $p < .001$).

JNeurosci Accepted Manuscript

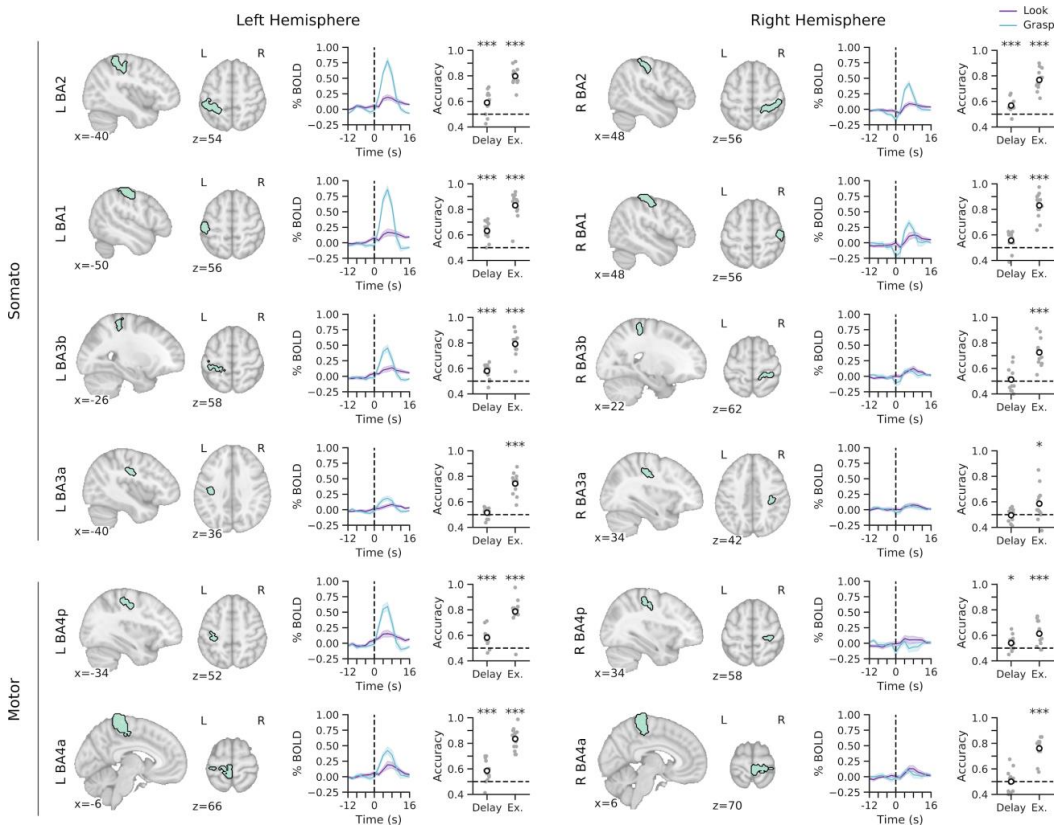

Figure 3. Experiment 2 decoding of motor effector information (right hand versus eye) from early somatosensory cortex during the delay epoch. Data is plotted and computed in the same way as in Figure 2, but for Experiment 2 data.

As in Experiment 1, it is useful to interpret these above decoding results in somatosensory cortex with respect to decoding in M1, known to differentiate the planning of hand versus eye movements in humans (Gallivan et al., 2011a). Notably, here we observed a similar pattern of effects in the motor cortex to that observed in BA3b. Specifically, we found significant decoding in the contralateral left primary motor ROIs, that was either absent or weaker in the ipsilateral right primary motor ROIs (*Left hemisphere*: BA4a: mean = 58.46%, $p < .001$; BA4p: mean = 58.27%, $p < .001$; *Right hemisphere*: BA4a: mean = 50.00, $p = .521$; BA4p: $t_{12} = 54.04\%$, $p = .033$, all p-values are FDR-corrected; see Fig 3). Again, decoding in both these areas was also significant during the Execute epoch (decoding accuracies between 61% - 83%; all $p < .001$). In sum, this result suggests that the motor effector information that can be decoded from BA3b (S1 proper) prior to movement is qualitatively (and topographically) similar to that which can be decoded from primary motor cortex.

JNeurosci Accepted Manuscript

The results from Experiment 2, when taken together, support our main observation from Experiment 1 that somatosensory cortex contains motor effector information prior to movement execution. Moreover, the finding that only left BA3b shows significant decoding of the upcoming movement, in which its decoding accuracies are also significantly greater than in right BA3b (t_{12} = 2.28, p = .042; paired t-test), suggests that movement planning information is represented in S1 proper in a contralateral fashion. Meanwhile, at the slightly higher-levels of somatosensory cortex, in BA1 and BA2, this information is represented in a bilateral fashion. The fact that motor effector decoding was only observed in contralateral BA3b during planning but was observed bilaterally in BA3b during execution may suggest separate gating mechanisms for planning versus execution at the earliest levels of somatosensory cortex.

Searchlight analyses in Experiments 1 and 2 reveal the contralateral nature of planning-related modulations in somatosensory cortex

To complement our above ROI analyses and bolster our observations from both Experiments 1 and 2, we also performed separate searchlight analyses in both data sets, with a focus on decoding along the postcentral and precentral gyri (see Methods). The presence or absence of spatial smoothing (see Methods) did not affect the overall pattern of results of our searchlight analyses in both Experiments 1 and 2. As such, we focus on the results of the smoothed searchlight analyses (see Fig 4A,B). During the Delay epoch in Experiment 1, the searchlight revealed large clusters in the left and right hemispheres that span all all somatosensory and motor areas used in the ROI analyses, as well as within supplemental motor cortex (Table 1, Experiment 1 for cluster information). Together, these clusters shared the greatest degree of overlap with BA1, BA3b, and BA4p in both hemispheres (see yellow bar plots in Fig. 4C). Upon movement execution, the majority of bilateral postcentral and precentral gyri exhibit decoding (see Fig. 4D).

JNeurosci Accepted Manuscript

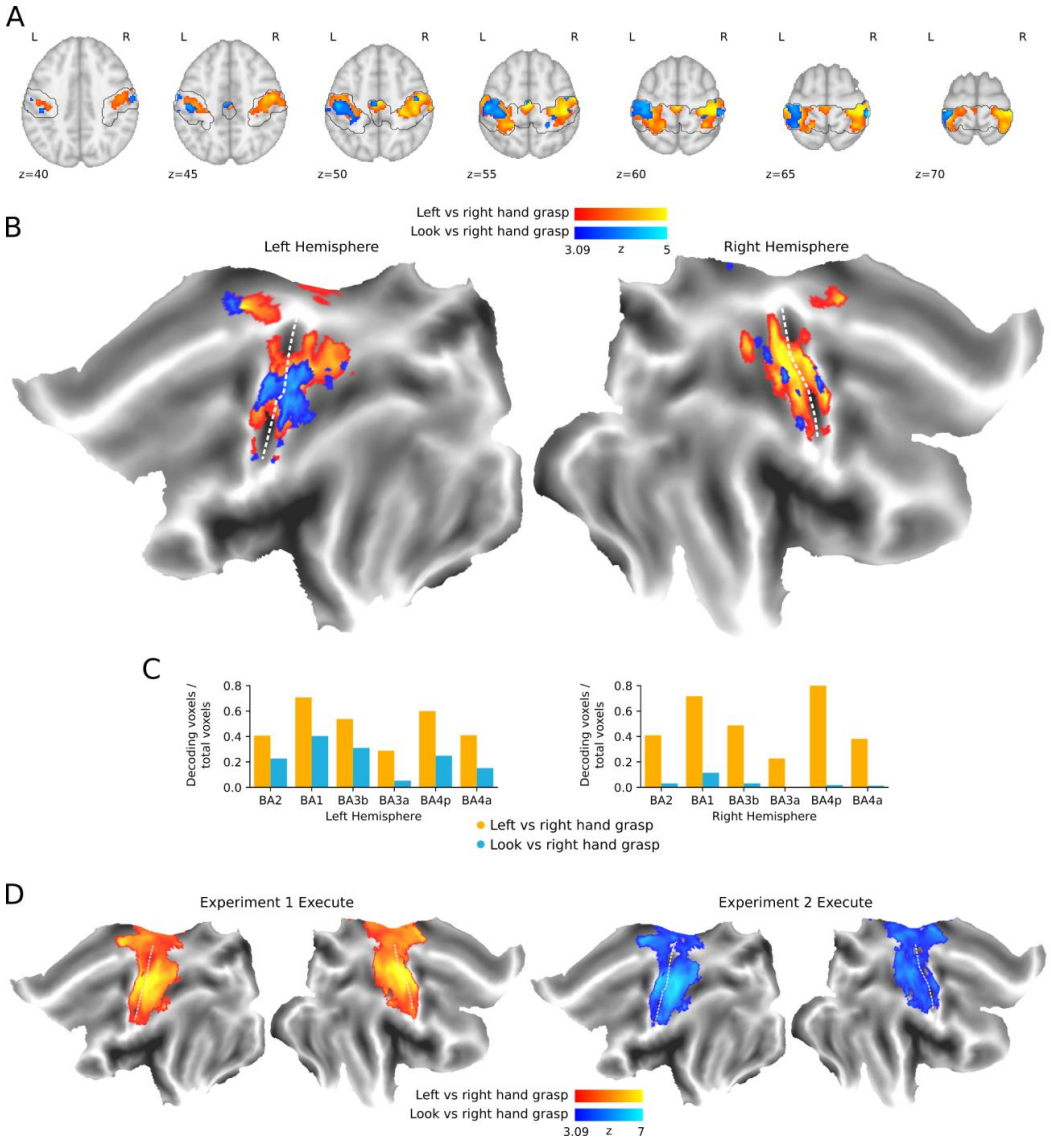

Figure 4. Searchlight analyses show that the encoding of motor effector information during planning in Experiment 1 (when both hands are used) occurs in bilateral S1 (and M1) whereas, in Experiment 2 (when only one hand is used), it primarily occurs in contralateral S1 (and M1). Searchlight analyses were restricted to a mask encompassing all somatosensory and motor ROIs. Group-level searchlight maps were thresholded at z = 3.09 (one-tailed $p < .001$) and cluster-corrected at $p < .05$ based on permutation procedures (see Methods). **A.** Axial slices of Experiment 1 (orange-yellow) and Experiment 2 (blue) searchlight maps. Black trace shows the boundaries of the searchlight mask. **B.** Searchlight results projected onto flat surface maps. White dashed lines denote the central sulcus in each hemisphere. **C.** Proportion of significant decoding voxels for left and right hemisphere ROIs,

JNeurosci Accepted Manuscript

computed by taking the number of voxels belonging to searchlight clusters ("decoding voxels") within an ROI and dividing by the total number of voxels within that ROI. **D.** Searchlight results of the Execute epochs in Experiment 1 (left) and 2 (right).

[INSERT TABLE 1 HERE]

During the Delay epoch in Experiment 2, we observed a large searchlight cluster in the left hemisphere situated predominantly on the postcentral gyrus but also extending into the precentral gyrus, along with additional clusters in supplementary motor cortex and inferolateral precentral gyrus (see Table 1, Experiment 2 clusters 4, 6, 7; Figure 4A,B). Meanwhile, the right hemisphere showed smaller clusters along precentral and postcentral gyri, primarily in BA1 (see Table 1, Experiment 2 clusters 2-5, 8-9). Although the clusters in the left hemisphere had substantial overlap with the left ROIs, clusters in the right hemisphere occupied only a marginal number of voxels, if any, with the right ROIs (see blue bar plots in Fig 4C). Overall, these findings are largely consistent with our observations in the ROI decoding analyses in that the searchlight demonstrates a striking contralateral (left) hemisphere bias, with BA1 showing the largest degree of bilateral decoding. Similar to Experiment 1, bilateral postcentral and precentral gyri exhibit decoding during movement execution (see Fig. 4D). The convergence of our ROI findings and searchlight results is also important in terms of identifying constraints on the sensitivity of the MVPA approach; that is, motor effector decoding in Experiment 2 is not simply found everywhere throughout S1 and M1 (as in Experiment 1), but rather it is largely confined to the contralateral hemisphere. For completeness, we also show these Delay epoch decoding results in Experiment 1 and 2 in the context of the different effector activations (univariate contrast maps) elicited during movement execution (see Figure 5).

JNeurosci Accepted Manuscript

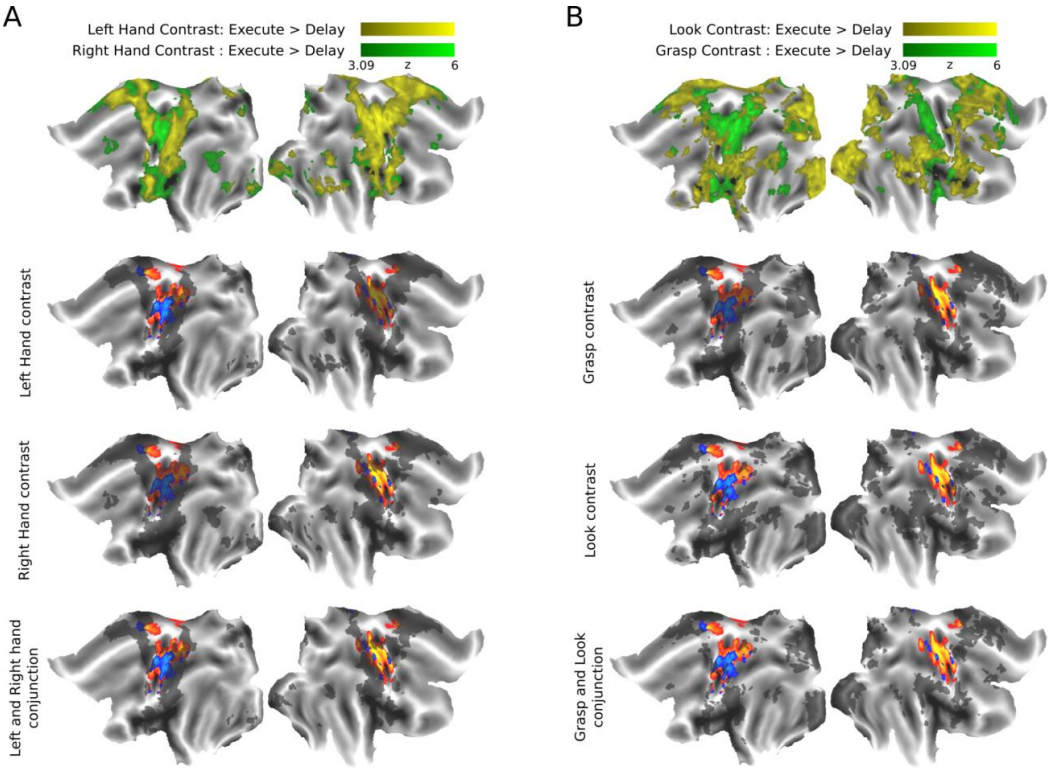

Figure 5. Searchlight results in context of activity produced by the execution of each effector in Experiment 1 and 2. A. Top panel shows the univariate contrast maps of individual Execute vs Delay contrasts for Left (yellow) and Right (green) hand (see Methods). Each contrast map was thresholded at $p < .001$ and cluster corrected ($p < .05$, using AFNI's 3dClustSim). Shaded regions in the three panels below show the overlay of each univariate contrast map, as well as their conjunction (bottom), onto the searchlight results displayed in Fig 4B (Orange = Experiment 1: Left vs Right Hand decoding; Blue = Experiment 2: Look vs Grasp decoding). **B.** Same as A, but for Experiment 2 Execute > Delay contrast (yellow = Look contrast; green = Grasp contrast).

DISCUSSION

Here, we asked whether the motor effector used in an upcoming action can be decoded, prior to movement, from neural activity patterns in S1. Experiment 1 showed that the planning of left versus right hand movements could be decoded from pre-movement activity in both left and right subfields of S1 (BA3a, BA3b, BA1 and BA2). Experiment 1 findings were replicated in Experiment 2, wherein participants prepared object-directed movements of the right hand versus eye. However, we additionally showed that effector decoding differed across subareas, with decoding in higher-order somatosensory regions (BA1 and BA2) occurring bilaterally (i.e.,

JNeurosci Accepted Manuscript

in both the left and right hemispheres) and the decoding in lower-order S1 proper (BA3b) occurring contralaterally to the hand. Our S1 results in both experiments paralleled the decoding in primary motor cortex, suggesting that motor effector information was present in both the somatosensory and motor cortices. Together, these experiments suggest that motor planning, in addition to preparing the motor system for movement, involves changing the neural state of the somatosensory system, presumably allowing it to anticipate the cutaneous signals that arise during movement execution.

Pre-movement modulations of neural activity have been widely reported throughout the cortical motor system (Churchland et al., 2010a; Gallivan and Culham, 2015b). Traditionally, through the single-neuron recording approach, these modulations have been interpreted as reflecting the coding of various movement parameters (e.g., direction), wherein this activity is thought to represent a subthreshold version of the upcoming movement to be executed (for review, see Churchland et al., 2010a). More recently, neural recordings performed at the population level (via multi-unit arrays) argue that this modulation reflects a state transition that brings population activity to a point at which movement execution unfolds naturally through intrinsic neural processes (Churchland et al., 2010b, 2012; Shenoy et al., 2013; Sussillo et al., 2015; Pandarinath et al., 2017; Lara et al., 2018). Despite key differences in these two frameworks, they both interpret the pre-movement modulations as some form of ‘motor preparation’, and attempt to explain this activity in the context of descending spinal motor commands (Churchland et al., 2010c; Russo et al., 2018). By contrast, what might the preparatory activity in S1 represent?

One possibility is that S1 actually has some level of control over the upcoming hand actions. There is evidence from rodents that S1 (barrel cortex) can directly control whisker movements via innervation of motoneurons through the spinal trigeminal nuclei (Matyas et al., 2010). Similarly, there is evidence in NHPs that S1 has descending projections that terminate in the ventral horn of the spinal cord, where motoneurons are located (Rathelot and Strick, 2006). However, it is unlikely that these S1 projections in NHPs are directly involved in movement generation per se (Rathelot and Strick, 2006), given that S1 electrical stimulation has been rarely shown to evoke overt movements (Widener and Cheney, 1997). Rather, these descending S1 projections may exert an indirect contribution to motor control by synapsing on the gamma motoneurons that control the gain of muscle spindle afferents (Rathelot and Strick, 2006). In this way, S1 could contribute to the fine motor control of actions by changing the

JNeurosci Accepted Manuscript

sensitivity of the spindle afferents to optimally process limb and finger position during movement.

A second possibility is that S1 could be encoding proprioceptive information conveying the current state (e.g., position) of the limb. State estimation is a critical component to current theories of motor control (Scott, 2004), with recent work suggesting that limb-related proprioceptive information is encoded in primate somatosensory cortex (Chowdhury et al., 2020). With respect to movement planning, prior work has shown that proprioceptive signals are used directly to specify joint-based motor commands (Sober and Sabes, 2003; Sarlegna and Sainburg, 2009), which could partly explain why the loss of proprioceptive information can be so devastating for motor control (Sainburg et al., 1993; Teasdale et al., 1993). Given that different effectors were compared in our studies (i.e., left vs. right hand in Experiment 1 and right hand vs. eye in Experiment 2), the relevant state parameters would presumably change (or require updating) on a per trial basis, which could explain, at least in part, our S1 decoding results.

A third possibility is that the pre-movement modulation of S1 relates to some form of motor-related imagery. Recent single-unit recording work in a tetraplegic human patient has shown that S1 encodes imagined reaching movements, and that this coding is tuned to the imagined limb position (Jafari et al., 2020). This finding extends upon work in spinal cord injured patients showing that effector movement imagery engages distinct cortical neural populations in posterior parietal cortex that are also typically recruited during the actual movement of that effector (Aflalo et al., 2015; Zhang et al., 2017). Together, these patient findings suggest a role for S1 in motor imagery, and demonstrate that S1 can be engaged in the complete absence of sensation or even expected sensation. While the extent to which these observations in spinal cord injured patients generalize to neurologically healthy individuals is unclear (and thus whether they can account for the present results), our finding that distinct effector movements are represented in pre-movement S1 activity bolsters the emerging view from these patient studies that S1 is not simply a passive purveyor of tactile and proprioceptive information to cortex.

A fourth, and we think likely, possibility is that the pre-movement modulation of S1 observed here reflects predictive coding of the sensory consequences of the prepared movements. Such prediction is theorized to arise through an internal forward model (Miall and Wolpert, 1996), which provides the brain with an internal mechanism to disambiguate self-generated versus

JNeurosci Accepted Manuscript

externally generated sensory information (Wolpert and Flanagan, 2001). Studies focused on perceptual and/or sensory processing presume that the forward model has the effect of cancelling, or 'attenuating', the predictable sensory consequences of action (Bastos et al., 2012; Clark, 2013; Schneider and Mooney, 2018). Such 'sensory cancellation' phenomena have been well studied in the context of tasks involving manual interactions with objects, such as the attenuation of perceived force produced by self-generated movements compared to the same force being delivered externally (Shergill et al., 2003). Importantly, this attenuation is temporally tuned to the timing of the predicted contact event rather than linked to movement, per se (Bays et al., 2005, 2006). This is consistent with neural recording work in animals showing that neural activity in S1 is attenuated to a greater extent during, and prior to, voluntary movements of the limb as compared to passive movements of the same limb (Starr and Cohen, 1985; Jiang et al., 1990b; Seki and Fetz, 2012).

The forward model is also theorized to support real-time, accurate motor control, particularly in object manipulation tasks (Flanagan et al., 2006; Johansson and Flanagan, 2009). In such tasks, object-related 'contact events' (e.g., contact of the digits with the object) give rise to discrete sensory signals in multiple modalities (e.g., tactile, visual) that can be used to efficiently monitor task performance (Wolpert et al., 2011) and launch rapid corrective actions based on mismatches between the predicted and actual sensory signals of these contact events. These corrective actions are intelligent and are updated depending on the nature of the mismatch and phase of the task (Flanagan et al., 2006). We and others have thus argued that, outside the motor system, the preparation of manipulation tasks could also involve forming a 'sensory plan'; i.e., a predicted series of sensory signals, linked to contact events, that can be expected to arise as a function of known object properties and the outgoing motor commands (Johansson and Flanagan, 2009; Gale et al., 2021). If such 'sensory plans' are represented in S1, then how might they arise?

It is possible that motor cortex provides S1 with an efference copy of upcoming movement execution signals through known reciprocal connections between these regions (Nelson, 1987; London and Miller, 2013; Chowdhury et al., 2020). Recently, (Umeda et al., 2019)) performed simultaneous neural recordings in S1, M1 and an ensemble of afferent neurons in the dorsal root ganglion and found that pre-movement activity changes in S1 during reaching and grasping are largely accounted for by the activity of M1, with S1 encoding information about the forthcoming activity of forelimb muscles only slightly after M1. During movement execution, by

JNeurosci Accepted Manuscript

792 contrast, S1 activity reflected both motor cortex activity and afferent activity in the dorsal root
793 ganglion. Together, this NHP study not only supports our observation here in humans that S1
794 activity encodes the imminent action to be performed (prior to the arrival of sensory feedback),
795 but it also suggests that motor cortex is the origin of this pre-movement modulation.
796
797 Experiment 2 of the current study revealed decoding of motor effector information during
798 planning only in the contralateral (left) BA3b, whereas this decoding was bilateral in adjacent
799 areas BA1 and BA2. Classic work in nonhuman primates has demonstrated callosal
800 connections between the primary somatosensory cortices (Jones et al., 1975, 1979) and the
801 density of these connections varies according to subarea (Killackey et al., 1983). BA3b, or S1
802 proper, exhibits the lowest density of these interhemispheric connections, particularly in the
803 hand region, whereas BA1 and BA2 have increasingly denser interhemispheric connectivity
804 (Killackey et al., 1983). This pattern of callosal connections resembles the early visual system,
805 wherein the interhemispheric connection density increases in a stepwise fashion from lower-to-
806 higher order areas (i.e., from V1 to V2 to V3, etc.) (Newsome and Allman, 1980; Van Essen et
807 al., 1982). To speculate, the rostro-to-caudal increase of callosal connections in S1 (Killackey et
808 al., 1983) may provide the basis for the contra- to bilateral topography of motor effector
809 decoding across BA3b, BA1 and BA2 observed here. That is, for the hand, the bilateral
810 exchange of sensory prediction information related to upcoming movement may only occur in
811 the later stages of the serial processing chain (i.e., in BA1 and BA2).
812
813 Finally, we note that previous investigations using fMRI and similar delayed movement tasks,
814 we and others have not reported any pre-movement modulations in S1 (Gallivan et al., 2011a,
815 2011b, 2013b, 2016; Ariani et al., 2015, 2018; Gertz et al., 2017). For our part, this earlier work
816 often used activity in somatosensory cortex as a ‘negative control’; i.e., the lack of pre-
817 movement decoding in somatosensory cortex was consistent with the widely held notion that the
818 region only responds to sensory feedback (associated with movement execution). However, the
819 results of the current study suggest that our prior inability to detect pre-movement modulations
820 in S1 may have been due to our mislocalization of S1, which was based on motor execution
821 activity (e.g., Gallivan et al., 2011a), rather than the more precise cytoarchitectonic delineations
822 utilized here. In summary, this current study, when combined with our recent studies on
823 planning-related decoding in the early visual (Gallivan et al., 2019) and auditory (Gale et al.,
824 2021) systems, adds to mounting evidence that the early sensory cortices have direct access to
825 ongoing sensorimotor processes in the motor system.

JNeurosci Accepted Manuscript

Acknowledgements

This work was supported by operating grants from the Canadian Institutes of Health Research (CIHR) awarded to J.R.F. and J.P.G. (MOP126158). J.P.G. was supported by a Natural Sciences and Engineering Research Council (NSERC) Discovery Grant, as well as funding from the Canadian Foundation for Innovation. D.J.G. was supported by a R.S. McLaughlin Fellowship and an NSERC graduate fellowship. The authors would like to thank Martin York, Sean Hickman, and Don O'Brien for technical assistance.

Author Contributions

J.R.F., and J.P.G. designed the experiments. D.J.G. and J.P.G. performed research. D.J.G. analyzed the data. D.J.G., J.R.F and J.P.G interpreted the data and wrote the paper. All authors provided edits and feedback on the final version of the paper.

Competing Interests Statement

The authors declare no competing financial interests.

JNeurosci Accepted Manuscript

REFERENCES

Abraham A, Pedregosa F, Eickenberg M, Gervais P, Mueller A, Kossaifi J, Gramfort A, Thirion B, Varoquaux G (2014) Machine learning for neuroimaging with scikit-learn. Front Neuroinform 8:14.

Aflalo T, Kellis S, Klaes C, Lee B, Shi Y, Pejsa K, Shanfield K, Hayes-Jackson S, Aisen M, Heck C, Liu C, Andersen RA (2015) Neurophysiology. Decoding motor imagery from the posterior parietal cortex of a tetraplegic human. Science 348:906–910.

Afshar A, Santhanam G, Yu BM, Ryu SI, Sahani M, Shenoy KV (2011) Single-trial neural correlates of arm movement preparation. Neuron 71:555–564.

Ames KC, Ryu SI, Shenoy KV (2014) Neural dynamics of reaching following incorrect or absent motor preparation. Neuron 81:438–451.

Ariani G, Oosterhof NN, Lingnau A (2018) Time-resolved decoding of planned delayed and immediate prehension movements. Cortex 99:330–345.

Ariani G, Wurm MF, Lingnau A (2015) Decoding Internally and Externally Driven Movement Plans. J Neurosci 35:14160–14171.

Avants BB, Epstein CL, Grossman M, Gee JC (2008) Symmetric diffeomorphic image registration with cross-correlation: evaluating automated labeling of elderly and neurodegenerative brain. Med Image Anal 12:26–41.

Bastos AM, Usrey WM, Adams RA, Mangun GR, Fries P, Friston KJ (2012) Canonical microcircuits for predictive coding. Neuron 76:695–711.

Batista AP, Santhanam G, Yu BM, Ryu SI, Afshar A, Shenoy KV (2007) Reference Frames for Reach Planning in Macaque Dorsal Premotor Cortex. Journal of Neurophysiology 98:966–983 Available at: http://dx.doi.org/10.1152/jn.00421.2006.

Bays PM, Flanagan JR, Wolpert DM (2006) Attenuation of self-generated tactile sensations is predictive, not postdictive. PLoS Biol 4:e28.

Bays PM, Wolpert DM, Flanagan JR (2005) Perception of the consequences of self-action is temporally tuned and event driven. Curr Biol 15:1125–1128.

Borich MR, Brodie SM, Gray WA, Ionta S, Boyd LA (2015) Understanding the role of the primary somatosensory cortex: Opportunities for rehabilitation. Neuropsychologia 79:246–255.

Brodmann K (1909) Vergleichende Lokalisationslehre der Grosshirnrinde in ihren Prinzipien dargestellt auf Grund des Zellenbaues von Dr. K. Brodmann,..

Burton H, Fabri M (1995) Ipsilateral intracortical connections of physiologically defined cutaneous representations in areas 3b and 1 of macaque monkeys: projections in the vicinity of the central sulcus. J Comp Neurol 355:508–538.

Cauller LJ, Clancy B, Connors BW (1998) Backward cortical projections to primary somatosensory cortex in rats extend long horizontal axons in layer I. J Comp Neurol 390:297–310.

JNeurosci Accepted Manuscript

879 Chowdhury RH, Glaser JI, Miller LE (2020) Area 2 of primary somatosensory cortex encodes
880 kinematics of the whole arm. Elife 9 Available at: http://dx.doi.org/10.7554/eLife.48198.

881 Churchland MM, Afshar A, Shenoy KV (2006a) A central source of movement variability.
882 Neuron 52:1085–1096.

883 Churchland MM, Cunningham JP, Kaufman MT, Foster JD, Nuyujukian P, Ryu SI, Shenoy KV
884 (2012) Neural population dynamics during reaching. Nature 487:51–56.

885 Churchland MM, Cunningham JP, Kaufman MT, Ryu SI, Shenoy KV (2010a) Cortical
886 preparatory activity: representation of movement or first cog in a dynamical machine?
887 Neuron 68:387–400.

888 Churchland MM, Cunningham JP, Kaufman MT, Ryu SI, Shenoy KV (2010b) Cortical
889 preparatory activity: representation of movement or first cog in a dynamical machine?
890 Neuron 68:387–400.

891 Churchland MM, Cunningham JP, Kaufman MT, Ryu SI, Shenoy KV (2010c) Cortical
892 preparatory activity: representation of movement or first cog in a dynamical machine?
893 Neuron 68:387–400.

894 Churchland MM, Santhanam G, Shenoy KV (2006b) Preparatory activity in premotor and motor
895 cortex reflects the speed of the upcoming reach. J Neurophysiol 96:3130–3146.

896 Churchland MM, Shenoy KV (2007) Delay of movement caused by disruption of cortical
897 preparatory activity. J Neurophysiol 97:348–359.

898 Cisek P, Crammond DJ, Kalaska JF (2003) Neural activity in primary motor and dorsal premotor
899 cortex in reaching tasks with the contralateral versus ipsilateral arm. J Neurophysiol
900 89:922–942.

901 Clark A (2013) Whatever next? Predictive brains, situated agents, and the future of cognitive
902 science. Behav Brain Sci 36:181–204.

903 Cox RW, Hyde JS (1997) Software tools for analysis and visualization of fMRI data. NMR
904 Biomed 10:171–178.

905 Crapse TB, Sommer MA (2008) Corollary discharge across the animal kingdom. Nat Rev
906 Neurosci 9:587–600.

907 Cui H, Andersen RA (2007) Posterior parietal cortex encodes autonomously selected motor
908 plans. Neuron 56:552–559.

909 Dale AM, Fischl B, Sereno MI (1999) Cortical surface-based analysis. I. Segmentation and
910 surface reconstruction. Neuroimage 9:179–194.

911 Darian-Smith C, Darian-Smith I, Burman K, Ratcliffe N (1993) Ipsilateral cortical projections to
912 areas 3a, 3b, and 4 in the macaque monkey. J Comp Neurol 335:200–213.

913 Eickhoff SB, Amunts K, Mohlberg H, Zilles K (2006a) The human parietal operculum. II.
914 Stereotaxic maps and correlation with functional imaging results. Cereb Cortex 16:268–
915 279.

JNeurosci Accepted Manuscript

916 Eickhoff SB, Grefkes C, Zilles K, Fink GR (2007) The somatotopic organization of
917 cytoarchitectonic areas on the human parietal operculum. Cereb Cortex 17:1800–1811.

918 Eickhoff SB, Schleicher A, Zilles K, Amunts K (2006b) The human parietal operculum. I.
919 Cytoarchitectonic mapping of subdivisions. Cereb Cortex 16:254–267.

920 Esteban O et al. (2019) nipy/nipype: 1.4.0. Available at: https://zenodo.org/record/3588470.

921 Esteban O, Markiewicz CJ, Blair RW, Moodie CA, Ilkay Isik A, Erramuzpe A, Kent JD,
922 Goncalves M, DuPre E, Snyder M, Oya H, Ghosh SS, Wright J, Durnez J, Poldrack RA,
923 Gorgolewski KJ (2018) fMRIPrep: a robust preprocessing pipeline for functional MRI. Nat
924 Methods:1.

925 Evans AC, Janke AL, Collins DL, Baillet S (2012) Brain templates and atlases. Neuroimage
926 62:911–922.

927 Fan R-E, Chang K-W, Hsieh C-J, Wang X-R, Lin C-J (2008) LIBLINEAR: A Library for Large
928 Linear Classification. J Mach Learn Res 9:1871–1874.

929 Fischl B, Sereno MI, Tootell RB, Dale AM (1999) High-resolution intersubject averaging and a
930 coordinate system for the cortical surface. Hum Brain Mapp 8:272–284.

931 Flanagan JR, Bowman MC, Johansson RS (2006) Control strategies in object manipulation
932 tasks. Curr Opin Neurobiol 16:650–659.

933 Gale DJ, Areshenkoff CN, Honda C, Johnsrude IS, Flanagan JR, Gallivan JP (2021) Motor
934 Planning Modulates Neural Activity Patterns in Early Human Auditory Cortex. Cereb Cortex
935 Available at: http://dx.doi.org/10.1093/cercor/bhaa403.

936 Gallivan JP, Chapman CS, Gale DJ, Flanagan JR, Culham JC (2019) Selective Modulation of
937 Early Visual Cortical Activity by Movement Intention. Cereb Cortex 29:4662–4678.

938 Gallivan JP, Culham JC (2015a) Neural coding within human brain areas involved in actions.
939 Curr Opin Neurobiol 33:141–149.

940 Gallivan JP, Culham JC (2015b) Neural coding within human brain areas involved in actions.
941 Curr Opin Neurobiol 33:141–149.

942 Gallivan JP, Johnsrude IS, Flanagan JR (2016) Planning Ahead: Object-Directed Sequential
943 Actions Decoded from Human Frontoparietal and Occipitotemporal Networks. Cereb Cortex
944 26:708–730.

945 Gallivan JP, McLean DA, Flanagan JR, Culham JC (2013a) Where one hand meets the other:
946 limb-specific and action-dependent movement plans decoded from preparatory signals in
947 single human frontoparietal brain areas. J Neurosci 33:1991–2008.

948 Gallivan JP, McLean DA, Smith FW, Culham JC (2011a) Decoding effector-dependent and
949 effector-independent movement intentions from human parieto-frontal brain activity. J
950 Neurosci 31:17149–17168.

951 Gallivan JP, McLean DA, Valyear KF, Culham JC (2013b) Decoding the neural mechanisms of
952 human tool use. Elife 2:e00425.

JNeurosci Accepted Manuscript

953 Gallivan JP, McLean DA, Valyear KF, Pettypiece CE, Culham JC (2011b) Decoding action
954 intentions from preparatory brain activity in human parieto-frontal networks. J Neurosci
955 31:9599–9610.

956 Gertz H, Lingnau A, Fiehler K (2017) Decoding Movement Goals from the Fronto-Parietal
957 Reach Network. Front Hum Neurosci 11:84.

958 Geyer S, Ledberg A, Schleicher A, Kinomura S, Schormann T, Bürgel U, Klingberg T, Larsson
959 J, Zilles K, Roland PE (1996) Two different areas within the primary motor cortex of man.
960 Nature 382:805–807.

961 Geyer S, Schleicher A, Zilles K (1999) Areas 3a, 3b, and 1 of human primary somatosensory
962 cortex. Neuroimage 10:63–83.

963 Gorgolewski K, Burns CD, Madison C, Clark D, Halchenko YO, Waskom ML, Ghosh SS (2011)
964 Nipype: a flexible, lightweight and extensible neuroimaging data processing framework in
965 python. Front Neuroinform 5:13.

966 Grefkes C, Geyer S, Schormann T, Roland P, Zilles K (2001) Human somatosensory area 2:
967 observer-independent cytoarchitectonic mapping, interindividual variability, and population
968 map. Neuroimage 14:617–631.

969 Greve DN, Fischl B (2009) Accurate and robust brain image alignment using boundary-based
970 registration. Neuroimage 48:63–72.

971 Haith AM, Pakpoor J, Krakauer JW (2016) Independence of Movement Preparation and
972 Movement Initiation. J Neurosci 36:3007–3015.

973 Hocherman S, Wise SP (1991) Effects of hand movement path on motor cortical activity in
974 awake, behaving rhesus monkeys. Exp Brain Res 83:285–302.

975 Holst E von, von Holst E, Mittelstaedt H (1950) Das Reafferenzprinzip. Naturwissenschaften
976 37:464–476 Available at: http://dx.doi.org/10.1007/bf00622503.

977 Huffman KJ, Krubitzer L (2001) Area 3a: topographic organization and cortical connections in
978 marmoset monkeys. Cereb Cortex 11:849–867.

979 Jafari M, Aflalo T, Chivukula S, Kellis SS, Salas MA, Norman SL, Pejsa K, Liu CY, Andersen RA
980 (2020) The human primary somatosensory cortex encodes imagined movement in the
981 absence of sensory information. Commun Biol 3:757.

982 Jenkinson M, Bannister P, Brady M, Smith S (2002) Improved optimization for the robust and
983 accurate linear registration and motion correction of brain images. Neuroimage 17:825–
984 841.

985 Jenkinson M, Beckmann CF, Behrens TEJ, Woolrich MW, Smith SM (2012) FSL. Neuroimage
986 62:782–790.

987 Jiang W, Chapman CE, Lamarre Y (1990a) Modulation of somatosensory evoked responses in
988 the primary somatosensory cortex produced by intracortical microstimulation of the motor
989 cortex in the monkey. Exp Brain Res 80:333–344.

990 Jiang W, Lamarre Y, Chapman CE (1990b) Modulation of cutaneous cortical evoked potentials

JNeurosci Accepted Manuscript

during isometric and isotonic contractions in the monkey. Brain Res 536:69–78.

Johansson, Flanagan JR (2009) Coding and use of tactile signals from the fingertips in object manipulation tasks. Nat Rev Neurosci 10:345–359.

Jones EG, Burton H, Porter R (1975) Commissural and cortico-cortical“ columns” in the somatic sensory cortex of primates. Science Available at: https://science.sciencemag.org/content/190/4214/572.abstract?casa_token=2obtpaNyquUAAAAA:dCLYY7m9FGoBj9oFHoTMjfZpjMzMXBMebB5dE-noj6wyLGmb1vGLrX6Phi-BxPyDeIb7rxgSE2Viwkw.

Jones EG, Coulter JD, Hendry SH (1978) Intracortical connectivity of architectonic fields in the somatic sensory, motor and parietal cortex of monkeys. J Comp Neurol 181:291–347.

Jones EG, Coulter JD, Wise SP (1979) Commissural columns in the sensory-motor cortex of monkeys. The Journal of Comparative Neurology 188:113–135 Available at: http://dx.doi.org/10.1002/cne.901880110.

Kaas JH (1983) What, if anything, is SI? Organization of first somatosensory area of cortex. Physiol Rev 63:206–231.

Kalaska JF (2009) From intention to action: motor cortex and the control of reaching movements. Adv Exp Med Biol 629:139–178.

Keele SW (1968) Movement control in skilled motor performance. Psychological Bulletin 70:387–403 Available at: http://dx.doi.org/10.1037/h0026739.

Khateb M, Schiller J, Schiller Y (2017) Feedforward motor information enhances somatosensory responses and sharpens angular tuning of rat S1 barrel cortex neurons. Elife 6 Available at: http://dx.doi.org/10.7554/eLife.21843.

Killackey HP, Gould HJ 3rd, Cusick CG, Pons TP, Kaas JH (1983) The relation of corpus callosum connections to architectonic fields and body surface maps in sensorimotor cortex of new and old world monkeys. J Comp Neurol 219:384–419.

Kinnischtzke AK, Simons DJ, Fanselow EE (2014) Motor cortex broadly engages excitatory and inhibitory neurons in somatosensory barrel cortex. Cereb Cortex 24:2237–2248.

Klapp ST, Erwin CI (1976) Relation between programming time and duration of the response being programmed. Journal of Experimental Psychology: Human Perception and Performance 2:591–598 Available at: http://dx.doi.org/10.1037/0096-1523.2.4.591.

Klein A, Ghosh SS, Bao FS, Giard J, Häme Y, Stavsky E, Lee N, Rossa B, Reuter M, Chaibub Neto E, Keshavan A (2017) Mindboggling morphometry of human brains. PLoS Comput Biol 13:e1005350.

Lanczos C (1964) Evaluation of Noisy Data. Journal of the Society for Industrial and Applied Mathematics Series B Numerical Analysis 1:76–85.

Lara, Elsayed GF, Zimnik AJ, Cunningham JP, Churchland MM (2018) Conservation of preparatory neural events in monkey motor cortex regardless of how movement is initiated. Elife 7 Available at: http://dx.doi.org/10.7554/eLife.31826.

JNeurosci Accepted Manuscript

1029 Lee S, Carvell GE, Simons DJ (2008) Motor modulation of afferent somatosensory circuits. Nat
1030 Neurosci 11:1430–1438.

1031 London BM, Miller LE (2013) Responses of somatosensory area 2 neurons to actively and
1032 passively generated limb movements. J Neurophysiol 109:1505–1513.

1033 Matyas F, Sreenivasan V, Marbach F, Wacongne C, Barsy B, Mateo C, Aronoff R, Petersen
1034 CCH (2010) Motor control by sensory cortex. Science 330:1240–1243.

1035 Messier J, Kalaska JF (2000) Covariation of primate dorsal premotor cell activity with direction
1036 and amplitude during a memorized-delay reaching task. J Neurophysiol 84:152–165.

1037 Miall RC, Wolpert DM (1996) Forward Models for Physiological Motor Control. Neural Networks
1038 9:1265–1279 Available at: http://dx.doi.org/10.1016/s0893-6080(96)00035-4.

1039 Miyashita E, Keller A, Asanuma H (1994) Input-output organization of the rat vibrissal motor
1040 cortex. Exp Brain Res 99:223–232.

1041 Mumford JA, Turner BO, Ashby FG, Poldrack RA (2012) Deconvolving BOLD activation in
1042 event-related designs for multivoxel pattern classification analyses. Neuroimage 59:2636–
1043 2643.

1044 Nelson RJ (1987) Activity of monkey primary somatosensory cortical neurons changes prior to
1045 active movement. Brain Res 406:402–407.

1046 Newsome WT, Allman JM (1980) Interhemispheric connections of visual cortex in the owl
1047 monkey, Aotus trivirgatus, and the bushbaby, Galago senegalensis. J Comp Neurol
1048 194:209–233.

1049 Niemi P, Näätänen R (1981) Foreperiod and simple reaction time. Psychol Bull 89:133–162.

1050 Pandarinath C, Nuyujukian P, Blabe CH, Sorice BL, Saab J, Willett FR, Hochberg LR, Shenoy
1051 KV, Henderson JM (2017) High performance communication by people with paralysis using
1052 an intracortical brain-computer interface. Elife 6 Available at:
1053 http://dx.doi.org/10.7554/eLife.18554.

1054 Pesaran B, Nelson MJ, Andersen RA (2006) Dorsal premotor neurons encode the relative
1055 position of the hand, eye, and goal during reach planning. Neuron 51:125–134.

1056 Pons TP, Kaas JH (1986) Corticocortical connections of area 2 of somatosensory cortex in
1057 macaque monkeys: a correlative anatomical and electrophysiological study. J Comp Neurol
1058 248:313–335.

1059 Porter LL, White EL (1983) Afferent and efferent pathways of the vibrissal region of primary
1060 motor cortex in the mouse. J Comp Neurol 214:279–289.

1061 Porter R, Lemon R (1995) Corticospinal Function and Voluntary Movement. Clarendon Press.

1062 Randolph M, Semmes J (1974) Behavioral consequences of selective subtotal ablations in the
1063 postcentral gyrus of Macaca mulatta. Brain Res 70:55–70.

1064 Rathelot J-A, Strick PL (2006) Muscle representation in the macaque motor cortex: an
1065 anatomical perspective. Proc Natl Acad Sci U S A 103:8257–8262.

JNeurosci Accepted Manuscript

1066 Riehle A, Requin J (1989) Monkey primary motor and premotor cortex: single-cell activity
1067 related to prior information about direction and extent of an intended movement. J
1068 Neurophysiol 61:534–549.

1069 Rosenbaum DA (1980) Human movement initiation: specification of arm, direction, and extent. J
1070 Exp Psychol Gen 109:444–474.

1071 Russo AA, Bittner SR, Perkins SM, Seely JS, London BM, Lara AH, Miri A, Marshall NJ, Kohn
1072 A, Jessell TM, Abbott LF, Cunningham JP, Churchland MM (2018) Motor Cortex Embeds
1073 Muscle-like Commands in an Untangled Population Response. Neuron 97:953–966.e8.

1074 Sainburg RL, Poizner H, Ghez C (1993) Loss of proprioception produces deficits in interjoint
1075 coordination. J Neurophysiol 70:2136–2147.

1076 Sarlegna FR, Sainburg RL (2009) The roles of vision and proprioception in the planning of
1077 reaching movements. Adv Exp Med Biol 629:317–335.

1078 Schneider DM, Mooney R (2018) How Movement Modulates Hearing. Annu Rev Neurosci
1079 41:553–572.

1080 Scott SH (2004) Optimal feedback control and the neural basis of volitional motor control. Nat
1081 Rev Neurosci 5:532–546.

1082 Seki K, Fetz EE (2012) Gating of sensory input at spinal and cortical levels during preparation
1083 and execution of voluntary movement. J Neurosci 32:890–902.

1084 Shen L, Alexander GE (1997) Preferential representation of instructed target location versus
1085 limb trajectory in dorsal premotor area. J Neurophysiol 77:1195–1212.

1086 Shenoy KV, Sahani M, Churchland MM (2013) Cortical control of arm movements: a dynamical
1087 systems perspective. Annu Rev Neurosci 36:337–359.

1088 Shergill SS, Bays PM, Frith CD, Wolpert DM (2003) Two eyes for an eye: the neuroscience of
1089 force escalation. Science 301:187.

1090 Snyder LH, Batista AP, Andersen RA (1997) Coding of intention in the posterior parietal cortex.
1091 Nature 386:167–170.

1092 Sober SJ, Sabes PN (2003) Multisensory integration during motor planning. J Neurosci
1093 23:6982–6992.

1094 Starr A, Cohen LG (1985) “Gating” of somatosensory evoked potentials begins before the onset
1095 of voluntary movement in man. Brain Research 348:183–186 Available at:
1096 http://dx.doi.org/10.1016/0006-8993(85)90377-4.

1097 Stelzer J, Chen Y, Turner R (2013) Statistical inference and multiple testing correction in
1098 classification-based multi-voxel pattern analysis (MVPA): random permutations and cluster
1099 size control. Neuroimage 65:69–82.

1100 Sussillo D, Churchland MM, Kaufman MT, Shenoy KV (2015) A neural network that finds a
1101 naturalistic solution for the production of muscle activity. Nat Neurosci 18:1025–1033.

1102 Tanji J, Evarts EV (1976) Anticipatory activity of motor cortex neurons in relation to direction of

JNeurosci Accepted Manuscript

1103 an intended movement. J Neurophysiol 39:1062–1068.

1104 Teasdale N, Forget R, Bard C, Paillard J, Fleury M, Lamarre Y (1993) The role of proprioceptive
1105 information for the production of isometric forces and for handwriting tasks. Acta Psychol
1106 82:179–191.

1107 Tustison NJ, Avants BB, Cook PA, Zheng Y, Egan A, Yushkevich PA, Gee JC (2010) N4ITK:
1108 improved N3 bias correction. IEEE Trans Med Imaging 29:1310–1320.

1109 Umeda T, Isa T, Nishimura Y (2019) The somatosensory cortex receives information about
1110 motor output. Sci Adv 5:eaaw5388.

1111 Van Essen DC, Newsome WT, Bixby JL (1982) The pattern of interhemispheric connections
1112 and its relationship to extrastriate visual areas in the macaque monkey. J Neurosci 2:265–
1113 283.

1114 Vogt BA, Pandya DN (1978) Cortico-cortical connections of somatic sensory cortex (areas 3, 1
1115 and 2) in the rhesus monkey. J Comp Neurol 177:179–191.

1116 Vogt C, Vogt O (1919) Journal Für Psychologie und Neurologie: Allgemeinere Ergebnisse
1117 unserer Hirnforschung.

1118 Widener GL, Cheney PD (1997) Effects on muscle activity from microstimuli applied to
1119 somatosensory and motor cortex during voluntary movement in the monkey. J
1120 Neurophysiol 77:2446–2465.

1121 Wolpert DM, Diedrichsen J, Flanagan JR (2011) Principles of sensorimotor learning. Nat Rev
1122 Neurosci 12:739–751.

1123 Wolpert DM, Flanagan JR (2001) Motor prediction. Current Biology 11:R729–R732 Available at:
1124 http://dx.doi.org/10.1016/s0960-9822(01)00432-8.

1125 Wong AL, Haith AM, Krakauer JW (2015) Motor Planning. Neuroscientist 21:385–398.

1126 Wu J, Ngo GH, Greve D, Li J, He T, Fischl B, Eickhoff SB, Yeo BTT (2018) Accurate nonlinear
1127 mapping between MNI volumetric and FreeSurfer surface coordinate systems. Hum Brain
1128 Mapp Available at: http://dx.doi.org/10.1002/hbm.24213.

1129 Zagha E, Casale AE, Sachdev RNS, McGinley MJ, McCormick DA (2013) Motor cortex
1130 feedback influences sensory processing by modulating network state. Neuron 79:567–578.

1131 Zhang CY, Aflalo T, Revechkis B, Rosario ER, Ouellette D, Pouratian N, Andersen RA (2017)
1132 Partially Mixed Selectivity in Human Posterior Parietal Association Cortex. Neuron 95:697–
1133 708.e4.

1134 Zhang Y, Brady M, Smith S (2001) Segmentation of brain MR images through a hidden Markov
1135 random field model and the expectation-maximization algorithm. IEEE Trans Med Imaging
1136 20:45–57.

1137

JNeurosci Accepted Manuscript

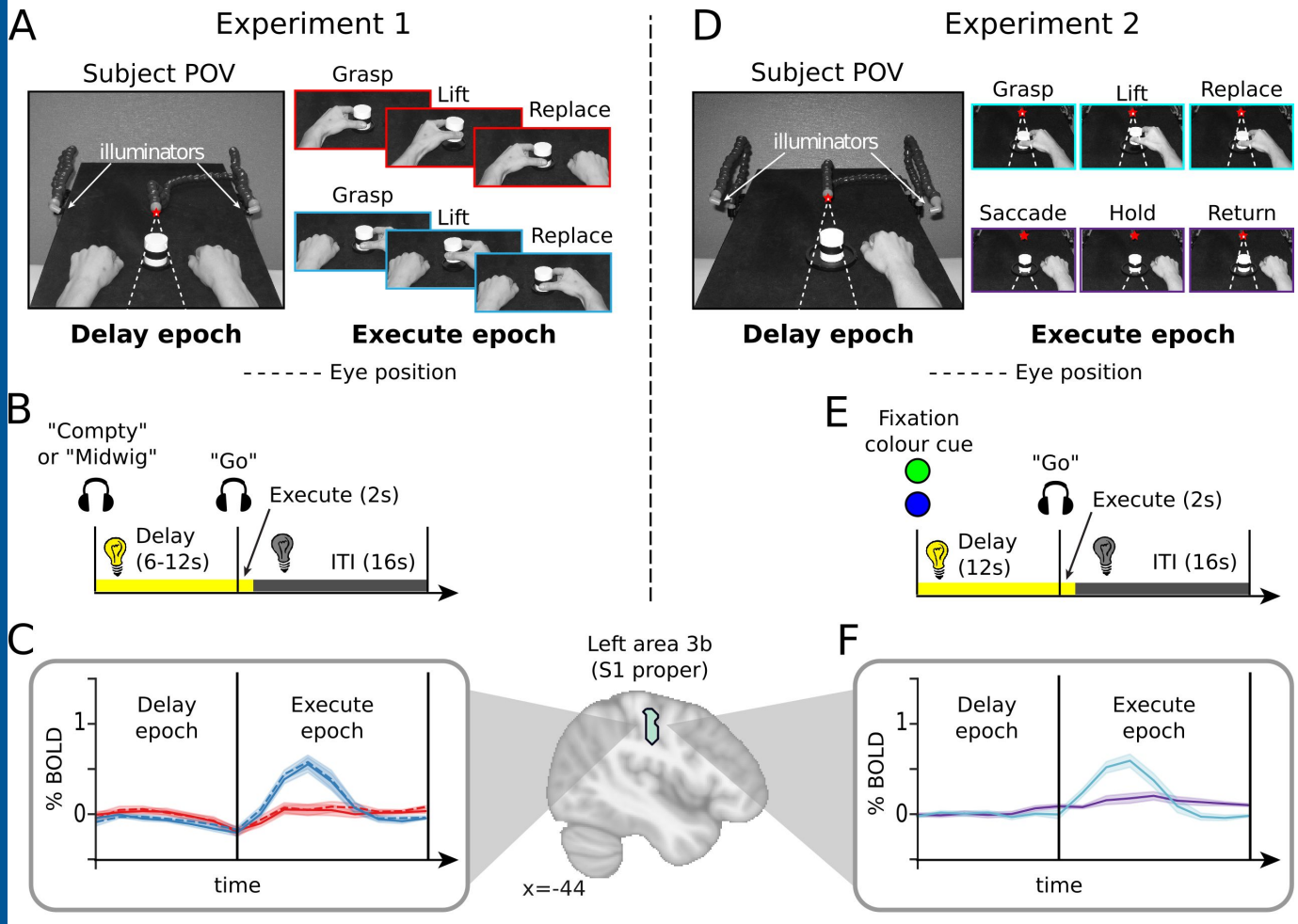

JNeurosci Accepted Manuscript

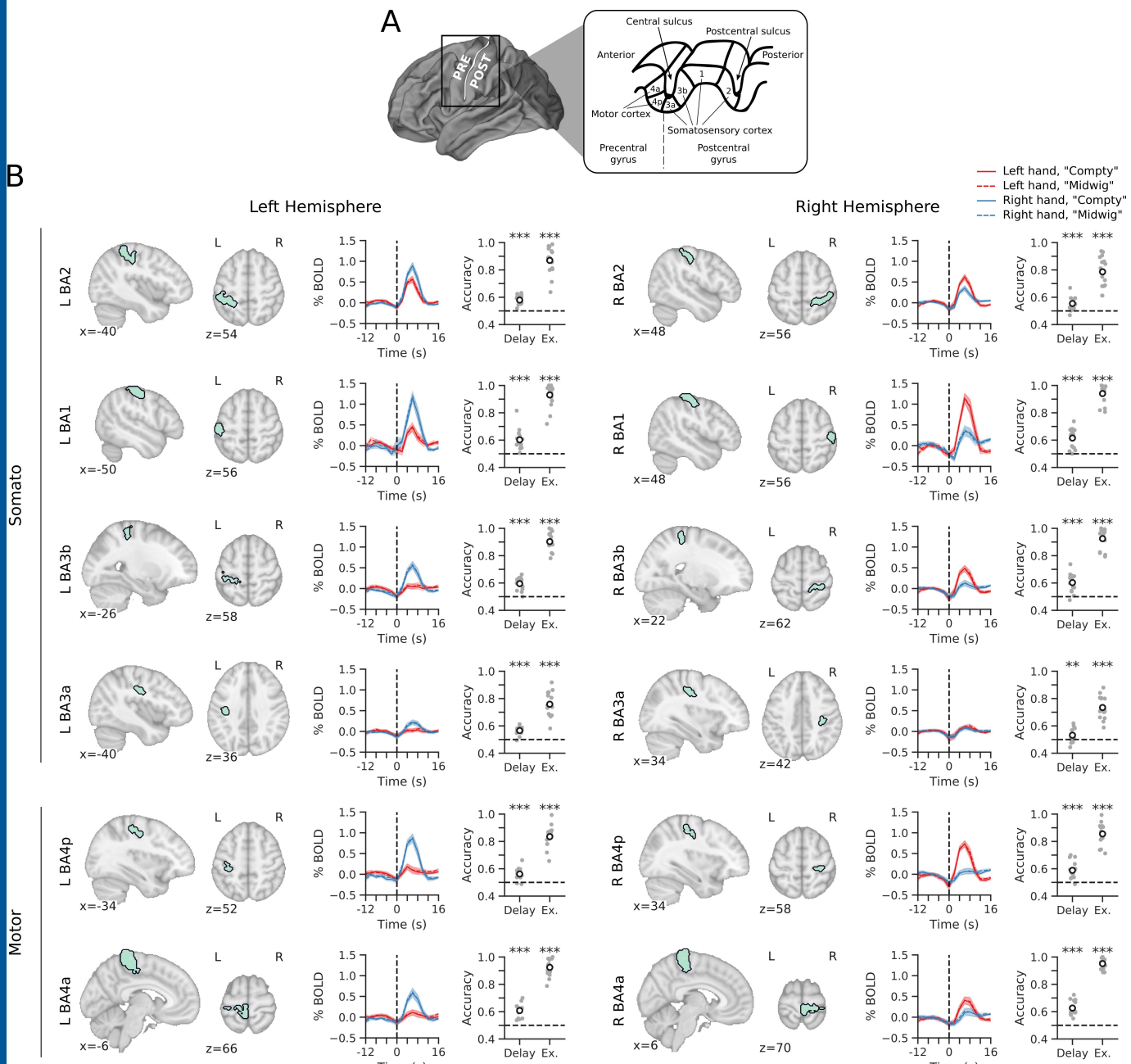

JNeurosci Accepted Manuscript

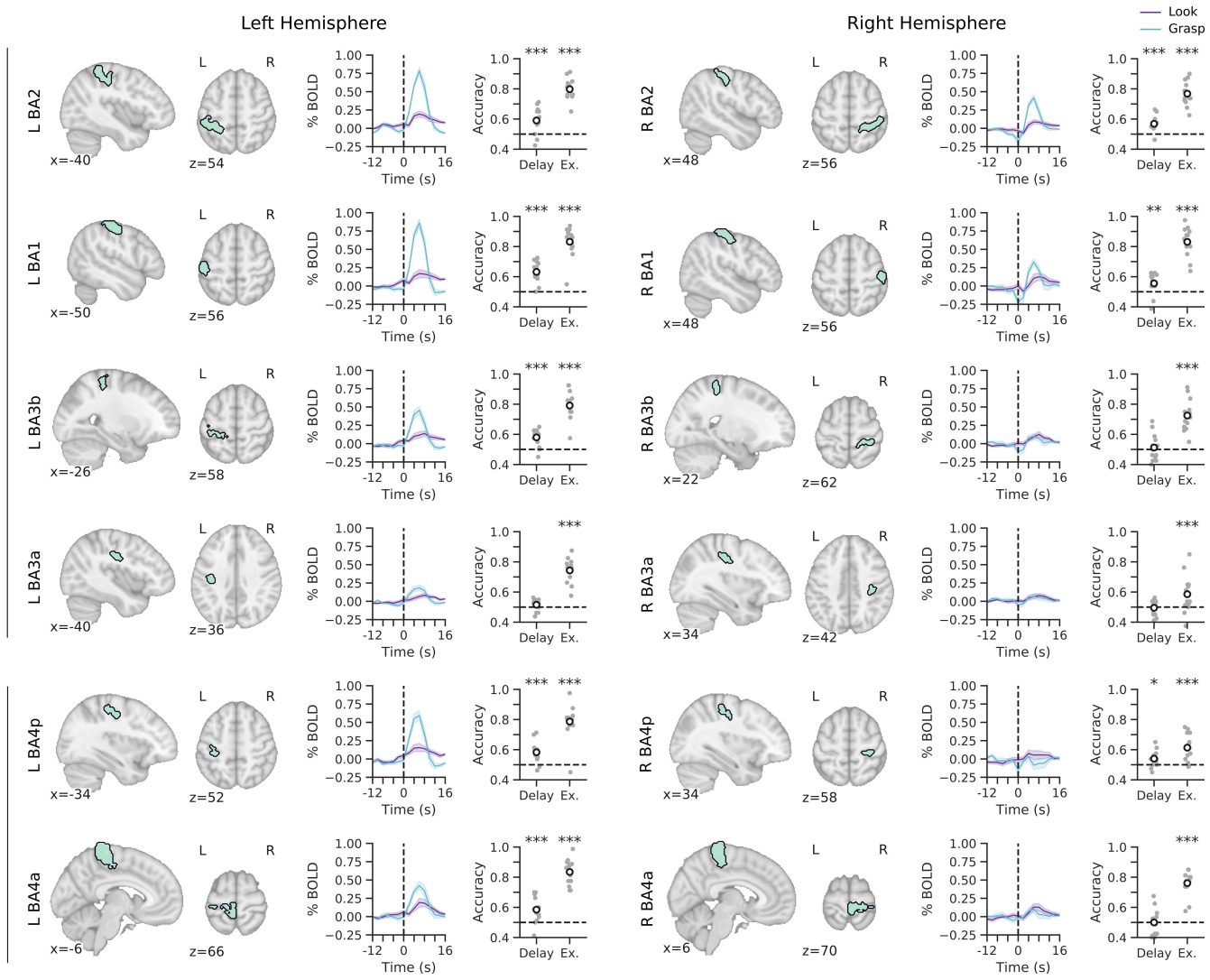

JNeurosci Accepted Manuscript

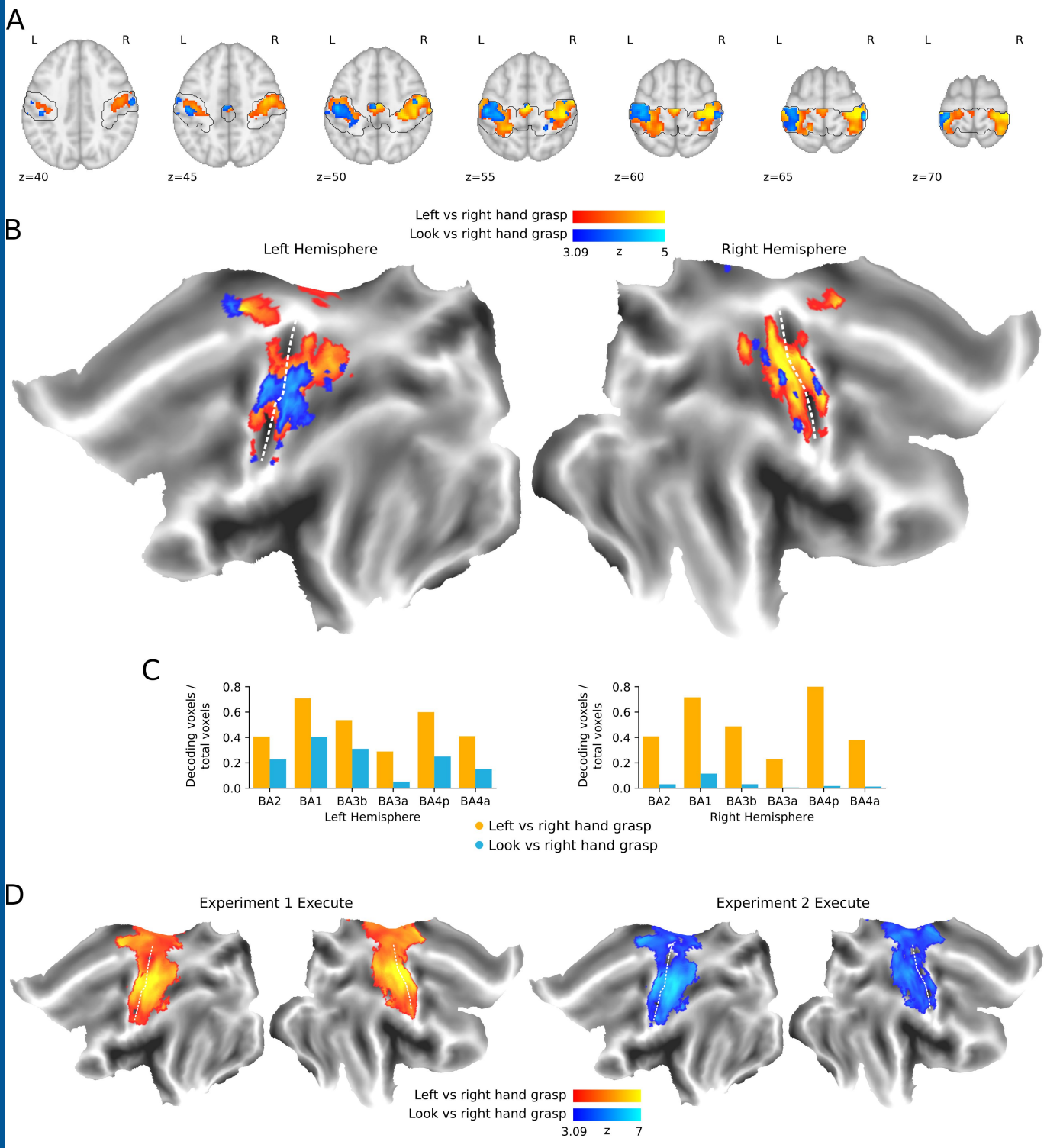

JNeurosci Accepted Manuscript

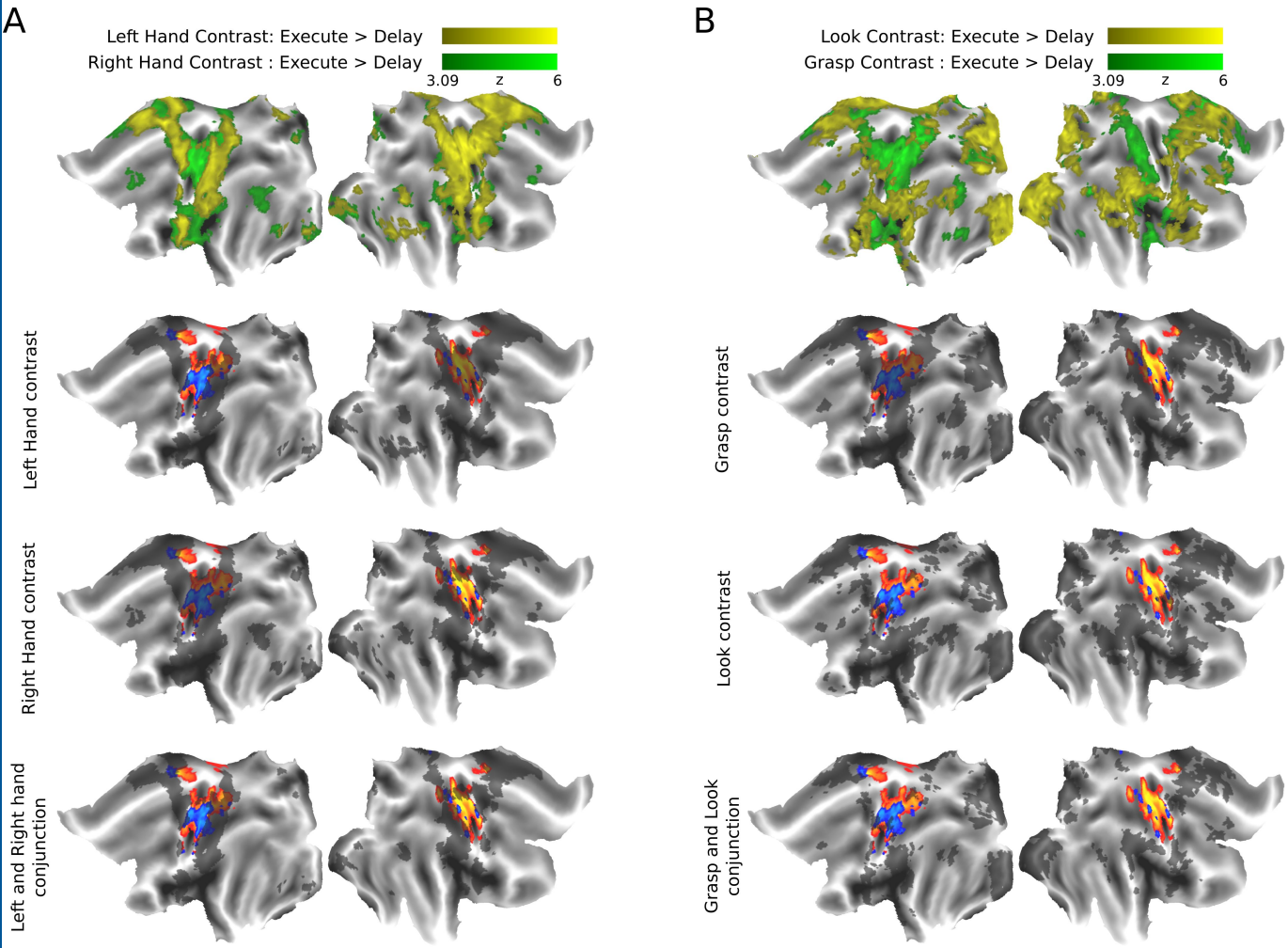

JNeurosci Accepted Manuscript

Table 1. Searchlight clusters in Experiments 1 and 2.

		Peak				
	Cluster	X	Y	Z	*z*	Size (mm^3)
Experiment 1	1	-36	-30	72	5.97	22248
	2	42	-28	56	5.59	22040
	3	0	-20	58	5.59	3440
	4	-60	-2	34	3.89	392
Experiment 2	1	-46	-22	54	4.88	9600
	2	-4	-18	46	4.00	624
	3	46	-30	64	4.8	568
	4	44	-12	52	4.27	360
	5	62	-12	40	3.85	304
	6	-62	-4	30	3.75	272
	7	-60	-10	44	3.53	272
	8	22	-42	56	3.85	248
	9	28	-34	58	3.72	216

Coordinates of each cluster's peak value (*z*) given in MNI152-space. Clusters are sorted by cluster size in descending order.